catalysts

MDPI

Review

Hydrogenation of Carbon Dioxide on Supported Rh Catalysts

András Erdőhelyi

Institute of Physical Chemistry and Materials Science, University of Szeged, Rerrich Béla tér 1, H-6720 Szeged, Hungary; erdohely@chem.u-szeged.hu; Tel.: +36-62-343-638; Fax: +36-62-546-482

Received: 14 December 2019; Accepted: 23 January 2020; Published: 29 January 2020

Abstract: The constant increase in the CO_2 concentration in the atmosphere requires us to look for opportunities to convert CO_2 into more valuable compounds. In this review, the activity and selectivity of different supported metal catalysts were compared in the hydrogenation of carbon dioxide, and found that Rh is one of the best samples. The possibility of the CO_2 dissociation on clean metal and on supported Rh was discussed separately. The hydrogenation of CO_2 produces mainly CH_4 and CO, but the selectivity of the reaction is affected by the support, in some cases the reduction of the support, the particle size of Rh, and the different additives. At higher pressure methanol, ethanol, and acetic acid could be also formed. The activity of the various supported Rh catalysts was compared and the results obtained for TiO_2-, SiO_2-, and Al_2O_3-supported catalysts were discussed in a separate chapter. The compounds formed on the surface of the catalysts during the reaction are shown in detail; mostly, different CO species, adsorbed formate groups, and different carbonates were detected. In a separate chapter the mechanism of the reaction was also discussed.

Keywords: supported Rh catalysts; hydrogenation of CO_2; CO_2 + H_2 reaction; methanation of CO_2

1. Introduction

The carbon dioxide concentration in the atmosphere increased dramatically since the industrial revolution. The levels of CO_2 in the atmosphere underwent slow fluctuations in the last few 100,000 years, but always remained below 300 ppm. In the last century, the burning of fossil fuels and new technologies (cement production, iron, steel industry etc.) have rapidly driven atmospheric CO_2 levels to new heights. In approximately 1910, the CO_2 concentration exceeded 300 ppm, in 2014 it reached 400 ppm, and now the CO_2 concentration is over 415 ppm [1,2]. According to lots of scientists the higher CO_2 concentration resulted in climate change, the rise in temperature. If we want to prevent the further increase of CO_2 concentration in the atmosphere we have to hinder the enhancement of the carbon dioxide emission and we need to increase the conversion of CO_2 to other more valuable compounds. The amount of all products that could be produced nowadays using CO_2 is only a few hundred Mt, whereas the carbon emission only from the large stationary sources is more than 10 Gt. It means that conventional products and technologies for CO_2 utilization do not influence the CO_2 concentration in the atmosphere.

This means that new procedures should be applied especially where CO_2 emissions are significant. The highest carbon emission sector is the energy industry and the transportation so we have to look for the solution in these fields.

Products that can be produced in the hydrogenation of carbon dioxide, methane, and methanol could be used directly either in the energy industry or in the transportation. Another important product is CO which is the component of synthesis gas and from it plenty of products can be produced including gasoline.

These processes could help the storage of electricity, too, whereas the greatest problem with the renewable energy (wind and solar) production is their fluctuation and the energy consumption is also uneven. The H_2 could come from the electrolysis of water and if the electricity has a renewable source on the one hand, then it is an environmentally friendly process, and on the other hand, by the conversion of products (for example burning of methane), the energy invested can be recovered. Extensive research work has been conducted on different catalytic systems for CO_2 conversion. Recently, various metal catalysts have been developed that demonstrated CO_2 methanation at low temperatures and atmospheric pressure.

Knowing the above, it is not surprising that the hydrogenation of carbon dioxide is in the focus of academic and industrial research again.

2. Hydrogenation of CO_2 on Supported Metal Catalysts

The CO_2 methanation was discovered by Sabatier and Senderens in 1902 [3], and has been investigated now and developed for more than a hundred years. A variety of different metals were used as catalysts in the CO_2 hydrogenation. The results obtained are summarized in different reviews [4–9]. Based on the metal catalysts' activities and selectivities, different activity orders have been published by different research groups. Analyzing these orders and the previous literature, the following order of activity for various metals in CO_2 methanation is revealed [10].

$$\text{Ru} > \text{Rh} > \text{Ni} > \text{Fe} > \text{Co} > \text{Os} > \text{Pt} > \text{Ir Mo} > \text{Pd} > \text{Ag}$$

Among these catalysts, Ru, Rh, and Ni exhibited the highest activity and selectivity.

Metal-promoted mesostructured silica nanoparticles have been studied for CO_2 methanation. The rate of methane formation (related to the metal content) was the highest on the Rh containing sample; however, on an area basis, Ni was the most active catalyst [11].

On alumina supported noble metal catalysts the activity order was Ru > Rh > Pt > Ir > Pd [12]. In another paper, it was found that the turnover frequency of CO_2 conversion on Rh supported on TiO_2 [13] was higher than on Ru samples but others found that Rh/Al_2O_3 activity exceeded only at higher temperatures the activity of Pt [14]. The highest CO_2 conversion was obtained on supported Rh compared with Pd and Ni catalysts supported on various oxides (SiO_2, Al_2O_3, and CeO_2) and zeolites (ZSM-5 and MCM-41) under the same experimental conditions [15].

The selectivity of methane formation depends strongly on the metal. It was significantly higher on Rh and Ru than on Pt and Pd. The methane selectivity was also the highest on Rh/Al_2O_3 and on Rh/CeO_2 followed by Ni/CeO_2. 2% Rh/PSAC (palm shell activated carbon) was also more active in the methanation of CO_2 than 2% Ni/PSAC [16].

Different metal-promoted mesostructured silica nanoparticles (MSN) have been studied for CO_2 methanation under atmospheric pressure. High activity was observed on Rh/MSN, Ru/MSN, Ni/MSN, and the CH_4 selectivity was 100% on Rh and Ru sample. However, on a metal basis, Rh/MSN was the most active catalyst, whereas Cu/MSN and Fe/MSN were the poorest samples [11].

The products formed in the CO_2 hydrogenation on different metals supported on zirconia depended strongly on the nature of the metal. Cu and Ag are suitable for methanol production, and Ni, Rh, and Ru yield methane. CH_4, CH_3OH, and CO formed on Pd, Re, Pt, and also on Au. In this case, Rh along with Pd, Au and Pt were considered less reactive metals [17].

The steady-state activity of CeO_2 supported noble metals were also compared [18]. According to these results, the catalyst can be divided into two groups: Ru and Rh, which give CH_4 only as the reaction product, and Pt, Pd, and Ir, which give mainly CO and the CH_4 selectivity was below 10%.

High-throughput screening methods were used for the heterogeneously catalyzed gas phase hydrogenation of CO and CO_2 over zirconia and ceria supported noble and base metal catalysts at 573–673 K and ambient pressure. Ru, Rh, and Ni were found to promote methanation, whereas Pt tends to catalyze the reverse water gas shift reaction. Methanation activity can be enhanced by some

acidic and redox dopants or suppressed by basic additives. However, Rh and Ru were the most active methanizers [19].

The brief summary above clearly shows that Rh is one of the best catalysts for CO_2 hydrogenation. Despite the high costs of rhodium, their superior catalytic properties at low temperature still make them indispensable to understand the interaction between the metal and the support, to check the surface compounds formed during the reaction and to show the elementary steps of the reaction.

3. Adsorption and Dissociation of CO_2 on Rh and on Supported Rh Catalysts

The adsorption and activation of CO_2 on Rh has also been widely investigated [20,21]. In the early studies, the adsorption of CO_2 was claimed to be weak and associative on Rh films [22], polycrystalline Rh [23], and alumina-supported Rh [24].

The Somorjai group [25–27] reported CO_2 dissociation on a Rh foil and on several Rh single crystal planes above critical CO_2 exposures, but Weinberg [28] and Goodman [29], on the basis of thermodynamic and kinetic results available at that time, indicated that the CO_2 sticking probability under the experimental conditions used (at low pressures and room temperature) would be by orders of magnitude smaller than needed to observe dissociation using surface analytical techniques like vibrational and thermal desorption spectroscopy (TDS). It was found that CO_2 adsorbed on the (111) and (110) faces of Rh single crystal at 100 K completely desorbs below 300 K without detectable dissociation [30,31]. However, deposition of potassium adatoms, an electron-donating promoter, on the Rh (111) surface activated the CO_2 molecule and caused its dissociation even at 150–200 K [32,33].

Using field electron microscopy (FEM), the Nieuwenhuys group [34,35] demonstrated that the crystallography of the surface Rh field emitter tip influenced the adsorption and dissociation of CO_2. By comparing TDS spectra with FEM patterns, a mechanism was proposed for the dissociative adsorption of CO_2 on Rh nanocrystals [34,35]. It was found the CO_2 dissociative adsorption to be the fastest on {012} facets [36].

On supported Rh catalysts the situation is basically different; the CO band appeared on the infrared spectra during CO_2 adsorption indicating the dissociation of CO_2, but it depends on the nature of the support [24,37–40]. Note that not everyone has noticed the appearance of CO bands after or during CO_2 adsorption, that is, the dissociation of CO_2 on supported Rh samples [41].

The preparation of the catalysts, the dispersity of Rh, the nature of the support, the adsorption temperature, and the CO_2 pressure all have an influence on this process.

The most effective support was TiO_2 but even on these samples the CO_2 dissociation was detected only above 373 K [37,38]. It was found that on Rh/TiO_2 reduced at 673 K CO formation was observed already at 423 K, but when this sample was reduced at 473 K, the dissociation was also observed at 423 K but only after 20 min of adsorption [42]. It means that the CO_2 dissociation depends on the reduction temperature of the TiO_2 supported samples, which could be attributed to the formation of oxygen vacancies on the perimeter of the Rh-TiO_2 interface during the reduction.

The CO_2 dissociation occurs on Rh/TiNT (titanate nanotube) and Rh/TiNW (titanate nanowire) at 493 K but at smaller extent than on Rh/TiO_2 under the same experimental conditions [43]. Other authors found that the CO_2 dissociation at room temperature does not occur; CO band was not detected on Rh/TiNT [44].

The interaction of CO_2 with Rh/TiO_2 (anatase) at 508 K results in the development of CO band at 1917 cm^{-1} assigned to the bridge bonded CO indicating the CO_2 dissociation. When the TiO_2 was doped with W^{6+}, the CO band intensity increased with increasing the dopant concentration and at 0.45 at% W^{6+} the linearly bonded CO is also appeared on the spectra at 2043 cm^{-1} [45].

In the case of Rh/Al_2O_3, the dissociation of CO_2 to CO was also observed by infrared spectroscopy already at near room temperature [40,46,47], but others found that the dissociation occurs only at higher temperature above 373 K [48]. XPS measurements show that the CO_2 oxidized the Rh during the dissociative adsorption and this oxidation deactivates the catalyst [46,49].

The formation of CO band was also observed on Rh/ZrO_2 and Rh/MgO during CO_2 adsorption but the intensity of them was weaker. In this case, only a peak characteristic for linearly bonded CO was detected at lower wavenumber than recorded after CO adsorption from gas phase. This shift was explained by an earlier observation that the band frequency of CO stretching on Rh is a strong function of CO coverage [24] and so the low surface concentration of CO resulted the band shift [40].

Fisher and Bell compared the CO spectra obtained after CO adsorption with those registered during the CO_2 dissociation on Rh/SiO_2 [39]. Similar spectra were observed in both cases. After CO adsorption linearly bonded CO (2067–2039 cm^{-1}) and a broad feature centered at 1895–1856 cm^{-1} assigned as bridge bonded CO were found. The spectrum exhibits a shoulder at 1949 cm^{-1}, which was attributed to $Rh_2(CO)_3$ species. The bands in the CO region registered after CO_2 adsorption are similar to those seen for adsorbed CO, only the peaks shifted to lower wavenumber. It is a questionable whether the twin structure is formed in this case during the adsorption of CO, although other studies reported about the di-carbonyl formation on Rh/SiO_2, too [50,51]. The formation of twin structured CO or *gem*-di-carbonyl on Rh is explained as the Rh^0 is oxidized with the surface OH groups of the support during the CO adsorption leading to the formation of this $Rh^+(CO)_2$ complex [41,52]. According to others, as only linearly bonded CO species were found after CO_2 adsorption on different Rh catalysts, it was concluded that this CO species are not able to disaggregate the Rh clusters [47].

The interaction of CO_2 with Rh/CeO_2 was studied with temperature programmed desorption [18]. Significant differences were found in the behavior of the catalyst subjected to different reduction treatments; after reduction at 473 K, CO_2 was mainly desorbed and a small amount of CO was detected. The ratio of CO_2/CO in the desorbed gases was 10. By increasing the reduction temperature to 773 K, the presence of both CO and CO_2 was detected, and the ratio of desorbed CO_2 to CO was 3.3. It was found that, by increasing the reduction temperature, the reduction of the bulk CeO_2 increased, and this process is not promoted by the supported metal. The CO_2 could be activated on Ce^{3+} sites with the formation of CO and Ce^{3+} oxidized to Ce^{4+}. The presence of oxygen vacancies in the bulk will be an additional driving force for the reduction of CO_2 [18].

4. Reaction of CO_2 with H_2 on Unsupported Rh Catalysts

The CO_2 hydrogenation was studied on Rh foil [25]. It was found that the reaction rates at 700 Torr are nearly identical to those obtained on dispersed Rh catalysts, and it was approximately seven times higher than the CO hydrogenation rate at the same temperature, at 523 K. The oxygen pretreatment increases the $CO_2 + H_2$ reaction fivefold, acetylene pretreatment reduces the methane formation, but no chain growth was observed [25]. A similar effect of the pre-oxidation was found on Rh powder and on Rh ribbon [53]. Sub-monolayer deposit of titania on Rh foil increases the rate of CO_2 hydrogenation. The methane formation rate exhibits a maximum at Ti coverage of 0.5 ML, and this rate was 15 times higher than that over the unpromoted Rh surface [54]. The increase in the rate in the presence of titania was attributed to an interaction between the adsorbed CO released by CO_2 dissociation and Ti^{3+} ions located at the edge of TiO_x islands covering the surface [54].

The efficiency and selectivity of mesoporous (meso-Rh) and nanoporous Rh (NP-Rh) was compared in the hydrogenation of CO_2 [55]. At 673 K, on NP-Rh, only CO was formed but on meso-Rh the methane selectivity was 100%, and the latter catalyst exhibits a higher reaction rate. Highly efficient performance and selectivity for CH_4 formation are achieved due to controllable crystallinity, high porosity, high surface energy, and large atomic step distribution of the sample [55].

Recently, it was found that the RhCo porous nanospheres exhibited enhanced catalytic activity for the hydrogenation of CO_2 to form methanol [56]. The turnover frequency on this sample reached 612 h^{-1}, which was 6.1 and 2.5 times higher than that of Rh/C and RhCo nanoparticles, respectively. In situ XPS results revealed that negatively charged Rh atoms are on the surface which promoted the activation of CO_2 to generate $CO_2^{\delta-}$ and methoxy intermediates [56].

A comparative study of the catalytic activity of polycrystalline Rh foil with Rh/SiO_2 and $Rh/VO_x/SiO_2$ model catalysts was carried out using the CO_2 hydrogenation as test reaction. The samples

were prepared by the evaporation of the components in UHV. The VO_x promoted catalyst was more active than the unpromoted one, and the activity of Rh clusters on SiO_2 with a size of 1 to 2 nm was found to be on average 4 times for CO + H_2 and 27 times higher for CO_2 + H_2, as compared to the Rh foil. The higher activity of Rh/SiO_2 for CO_2 + H_2 as compared to CO + H_2 was explained by the differences in CO dissociation rates. The promotion effect of VO_x was attributed to the oxygen vacancies on VO_x which promote the dissociation of CO [57].

The hydrogenation of CO_2 was investigated over Rh foil decorated with sub monolayer quantities of different oxides [58]. With the exception of FeO_x all of the metal oxides investigated enhanced the rate of CH_4 formation and the rate of it passes through maximum with increasing metal oxide coverage. The extent of rate enhancement for CO_2 hydrogenation decreases in the order TiO_x of Lewis acid–base complexes between the oxygen and adsorbed CO or H_2CO and anionic vacancies present at the edge of the oxide metal boundary [58].

The deposition of vanadium oxide on Rh foil cause rate enhancement for CO_2 hydrogenation, the rate maximizes at 6 times that of the clean surface rate at a coverage of 0.6 ML. It was found that V^{2+} species are responsible for increasing the CH_4 formation rate, whereas the V^{2+} cations promote the dissociation of CO_2 to CO_s and O_s and of CO_s to C_s and O_s. The latter reaction is proposed to be critical for CH_4 formation [59].

5. Reaction of CO_2 with H_2 on Supported Rh Catalysts

The support exerted a significant influence on the activity and selectivity of Rh in the hydrogenation of CO_2. The reaction produced mainly CH_4 and CO. Using higher pressure methanol and ethanol production is favored [60–62]. Only a few papers report the formation of more than a trace amount of higher hydrocarbons [63,64]. Trovarelli et al. [64] found on Rh/TiO_2 and on Rh/Nb_2O_5 C_1–C_6 hydrocarbons and the amount of them follows the Anderson–Schulz–Flory statistic, whereas Nozaki et al. detected on Rh/Nb_2O_5 significant amounts of C_2 and C_3 (the C_{2+} selectivity at 623 K was 37%), but on Rh/TiO_2 only CH_4 was observed [63].

Comparing the specific rate of CO_2 consumption on Al_2O_3, TiO_2, and SiO_2 supported Rh it was found that the most effective support was TiO_2 and the least effective one was SiO_2 [65]. The turnover frequency was more than 20 times higher on Rh/TiO_2 than on Rh/SiO_2. The high efficiency of Rh/TiO_2 was explained to different extent of electronic interaction between the Rh and the support, influencing the bonding and the reactivity of surface species [65]. As TiO_2 is an n-type semiconductor, a much greater electronic interaction can be expected than with alumina or silica [66].

The reaction of CO_2 + H_2 and CO + H_2 was compared over Rh supported on ZrO_2, Al_2O_3, SiO_2, Nb_2O_5, and MgO. Among these catalysts, Rh/ZrO_2 was the most active and Rh/MgO was the least active one [67,68]. On Rh/ZrO_2 the CO_2 + H_2 reaction took place even at 323 K whereas the CO +H_2 reaction occurred only above 403 K. In the reaction of CO_2 + H_2 only CH_4 was formed up to 473 K but a small amount of CO was also detected above this temperature [68].

In the hydrogenation of CO Rh/Nb_2O_5 was more active than Rh/ZrO_2 but in all cases the CO_2 conversion was higher than that of CO [67]. The main product in the CO_2 + H_2 reaction at 10 bar on Rh/Nb_2O_5 and on Rh/ZrO_2 was methane but on Rh/TiO_2 a significant amount of methanol was also formed, the methanol selectivity at 513 K was 60.7% [61].

5.1. Reaction of CO_2 with H_2 on Titania-Supported Rh Catalysts

In the comparison of different supported Rh catalysts, Rh/TiO_2 was usually the most active sample.

The initial rate of CO_2 hydrogenation depends on the reduction temperature of the catalyst; it increased significantly with increasing reduction temperature (between 473 and 673 K), but after some seconds, it drastically decreased [42]. The maximum initial rate of the methane formation on the sample reduced at 673 K was about twice of that in the presence of Rh/TiO_2 reduced at 473 K, whereas, in the steady state, the CH_4 production was nearly the same. When the sample was treated with water or with CO_2 at the reaction temperature before introducing CO_2 + H_2 mixture, the initial excess in the

methane formation was completely missing. The promotion effect of the reduction temperature was explained by the formation of oxygen vacancies on the perimeter of the Rh/TiO_2 interface, which can be re-oxidized by the adsorption of CO_2 and H_2O [42].

The particle size of Rh on TiO_2 influenced the efficiency of the catalyst; the CH_4 formation rate related to the number of surface Rh atoms increases with increasing the particle size of Rh up to ca. 7 nm. Beyond this size, the rate did not change. Higher activation energies were obtained for catalysts with small particle size (2 nm) whereas for larger clusters (>7 nm) the activation energy was lower and did not change with the size (Table 1.) [69]. On the contrary, the CO formation rate increases with increasing the amount of isolated Rh sites on TiO_2 [70]. This suggested that the size of the Rh particles is a key factor in the selectivity of the catalyst. These experimental results obtained on Rh/TiO_2 were supported by DFT calculations [71].

The catalytic properties of Rh supported on TiO_2 as well as on titanate nanotube (TiNT) and nanowire (TiNW) formed in the hydrothermal conversion of titania were tested in the CO_2 hydrogenation at 493 K. The activity order of the catalysts at the beginning of the reaction decreased in the order Rh/TiNW > Rh/TiO_2 > Rh/TiNT. The conversion of CO_2 on Rh/TiO_2 and Rh/TiNT was relatively stable but on Rh/TiNW decreased significantly in time. Rh/TiO_2 displayed the highest steady state activity [43].

On Rh/TiNT at 363 K at atmospheric pressure, besides methane and CO, formic acid formation was detected in the $CO_2 + H_2$ reaction. The calculated turnover frequency for HCOOH formation was 7.210^{-2} h^{-1} [44]. It was proposed that the Na^+ content in TiNT plays an important role in the various carbonate formation processes. The reduced Rh/TiNT has the ability to form rhodium hydride complexes which can interact with bidentate carbonates to yield formate species and facilitates the further hydrogenation to formic acid [44]. This proposal was supported by the infrared spectroscopic results on Rh/MgO. In this case, the band characteristic for the bicarbonate species decreased and the formate band increased when the catalyst after CO_2 adsorption was treated with hydrogen at 373 K [37].

In the $CO_2 + H_2$ reaction, a dynamic decrease was observed in the rate of methane formation and increase of CO production on Rh/TiO_2 when the CO_2/H_2 ratios were greater than 1 [70].

The quantitative relationship between the concentration of isolated (iso) and nanoparticle-based (NP) Rh sites on TiO_2 and the selectivity of CO_2 hydrogenation toward CO and CH_4 formation was observed [70]. The relative fraction of these sites changes dynamically under reaction conditions from nanoparticles form isolated sites, and this process results in the unstable reactivity of the catalysts with higher Rh content under H_2-lean conditions in time. Ten percent CO_2 had no observable effect on site fractions; whereas 10% CO caused the Rh_{iso} sites to convert to Rh_{NP} sites, whereas CO can induce restructuring of Rh nanostructures, even at room temperature [71].

The Rh_{iso} sites controls the CO formation rate (TOF), whereas the Rh_{NP} controls the CH_4 production. Thus, selectivity of CO and CH_4 formation in CO_2 hydrogenation is controlled by the ratio of Rh_{iso} and Rh_{NP} sites [70].

Similar results were obtained on RhY zeolite [72]. CH_4 is the main product on this catalyst, because the surface concentration of CO on Rh particles is kept low by the CO induced disruption of Rh particles into atomically dispersed Rh. In the sample which was doped with Li, as adsorbed CO is accumulated on the surface of stable Rh particles, mainly CO production occurs.

Contrary to these observations on titanate nanotube supported Rh catalyst it was found that the intensity of the XPS peak (at 308.2 eV) characteristic of highly dispersed Rh gradually decreased and nearly completely vanished after 60 min of the $H_2 + CO_2$ (4:1) reaction at 498 K [43] indicating the agglomeration of Rh sites during the $CO_2 + H_2$ reaction.

The strong metal–support interaction was studied on CeO_2-, TiO_2-, and Nb_2O_5-supported Rh catalysts using CO_2 hydrogenation as a test reaction [73]. Tauster et al. [74] found and designated the phenomenon to strong metal–support interaction (SMSI) that high temperature hydrogen treatment of reducible oxides supported Pt–metals causes the reduction of the oxide and induced the migration

of the substoichiometric oxide on the metal particles which resulted in the decrease of the hydrogen adsorption capacity and the activity of the catalysts. On Rh/TiO_2, after high temperature reduction, a small positive effect was observed in the steady-state conditions, whereas Rh/Nb_2O_5 showed a remarkable decrease in activity and on Rh/CeO_2 ~50% reduction was recorded. When the reaction was studied with pulse technique under unsteady state conditions, a completely different behavior was observed. The initial activity of Rh/TiO_2 and Rh/Nb_2O_5 is totally suppressed after reduction at 773 K, whereas an enhancement was observed on Rh/CeO_2. The activity increase was explained by the formation of bulk vacancies in CeO_2. In the case of Rh/TiO_2 and Rh/Nb_2O_5, the samples lose their activity due to encapsulation by reduced oxides but the water and the oxygen formed in the CO_2 dissociation reoxidize the oxide [73].

In an earlier work, Christopher et al. reported the dynamic decrease in the rate of CH_4 production and increase in the rate of CO production when the CO_2:H_2 ratio was greater than 1. It was attributed to the changes in the particle size of Rh [70]. In situ X-ray absorption spectroscopy (XAS) on a 2% Rh/TiO_2 catalyst during the 20% CO_2:2% H_2 treatment showed no measurable difference between the reduced and the untreated catalysts, with a constant Rh–Rh coordination number. The XAS results were consistent with ex situ STEM images of 2% Rh/TiO_2 catalysts after reduction and 20% CO_2:2% H_2 treatment showed no evidence of Rh structural changes [75].

In situ spectroscopy and microscopy measurements show that the high concentration of adsorbates (HCO_x) on TiO_2 induces oxygen-vacancy formation, which facilitates the migration of the support covered by HCO_x species onto the metal. This adsorbate-mediated SMSI (A-SMSI) encapsulation state is stabilized against reoxidation by H_2O and modifies the reactivity of all the remaining exposed Rh sites, and appears to be comprehensive in covering Rh, but amorphous and permeable to reactants. Formation of the A-SMSI state induces a selectivity switch in the CO_2-reduction reaction from CH_4 production on bare Rh particles to CO production in the A-SMSI state, which effectively renders Rh less active for C–H bond formation. A similar effect was found between the influences of 20% CO_2:2% H_2 and formic acid treatments on the reactivity of Rh/TiO_2 catalysts. These observations suggested the existence of an A-SMSI state; a high coverage of HCO_x promotes the formation of oxygen vacancies at the TiO_2 surface, and thereby causes migration of the support onto Rh [75]. It is rare that a paper is valued in the same issue as in the present case [76].

When Rh/TiO_2 was prepared from $Rh(NO_3)_3$ and the sample was calcined at 1273 K, so the BET surface was low, ~8 m^2/g; the main product in the CO_2 hydrogenation was CO and the CH_4 selectivity was only ~30% [77]. The turnover frequency of methane formation increased significantly when W^{6+} ions were incorporated into the TiO_2 support [77]. Increasing the W^{6+} concentration increased the rate and selectivity of CH_4 formation and decreased the apparent activation energy of the reaction, but the donation did not influence the partial order of hydrogen and carbon dioxide [78,79]. The donation enhanced the electric conductivity of the oxide by one to two orders of magnitude. Doping the TiO_2 support with lower valence ions (Mg^{2+}, Al^{3+}), which hardly influenced the electron conductivity of the oxide, caused only little alteration in the specific activity of Rh. The effect of doping the support with W^{6+} ions was attributed to the enhanced electron transfer from the TiO_2 to the Rh which promotes the dissociation of CO [45,77,78]. There is another possible explanation for the promoting effect of W^{6+}. The hydrogen chemisorption is favored on doped catalyst; there is an increase in the concentration of surface hydrogen participating in the rate determining step.

It was found that the activation energy for CO formation is much lower than that for CO_2 methanation (Table 1), indicating that the dissociation of CO_2 to CO is easier than methanation. A reduction in the apparent activation energy was observed when Rh was supported on W^{6+}-doped TiO_2 [77,78], but the value does not depend on the dopant concentration [78].

When the inlet pressure was increased to 10 bar on Rh/TiO_2 significant amount of methanol (the selectivity was 60.7%) and ethanol were formed at 513 K in the CO_2 + H_2 reaction, but the selectivity decreased as the reaction temperature increased. When 3% Rh/TiO_2 was promoted with Na (Rh/Na

ratio was 1/1.5), the methanol selectivity decreased but that of ethanol increased; at 533 K it was 13.3% [61].

Significant amount of ethanol was formed at 47 kPa pressure on Se doped Rh/TiO_2 catalyst ($[Rh_{10}Se]/TiO_2$). The selectivity of it was 83% at 523 K although problems of deactivation of the catalyst exist. Ethanol was not produced under the same experimental conditions on other supported Rh clusters on different (Al_2O_3, MgO, and SiO_2) oxide supported $[Rh_{10}Se]$ samples [62,80]. Different factors were proposed to explain preferential ethanol synthesis: the structural effect of $[Rh_{10}Se]$ framework, the electronic effect of interstitial Se and the support effect of TiO_2 [80].

The CO_2 feedstock often contains trace amounts of sulfur compounds. The effect of sulfur on the methanation of CO_2 was studied on different supported Rh catalysts [81]. It was found that a trace amount of H_2S (22 ppm) can promote the reaction on TiO_2- and CeO_2-supported Rh, whereas on other supports, such as SiO_2, ZrO_2, and MgO, or when the H_2S concentration was higher (116 ppm), the contamination poisons the reaction. TPD and XPS results show that the sulfur built into the support and so the catalysts became more active as a result of the formation of new active sites at the interface between the Rh and the support [81].

5.2. Reaction of CO_2 with H_2 on Silica Supported Rh Catalysts

A comparative study shows that the rate of methane formation over Rh/SiO_2 was higher for CO_2 than for CO hydrogenation [39] and the activation energy for CO_2 hydrogenation was lower than that for CO hydrogenation similarly as it was found on Rh/Al_2O_3 [65].

The difference in Rh loading [82] and in the precursor of the metal [83] significantly changed the product selectivity on SiO_2 supported Rh. The main product was CO for the low-loaded catalyst, whereas CH_4 was dominantly produced on Rh/SiO_2 when the Rh content was more than 5% [60,65,82]. Over the catalysts prepared from acetate and nitrate the main product was CO, but it was CH_4 over the samples prepared from chloride precursor. The ratio of hydroxyl groups to Rh particles on SiO_2 surface-determined by XPS, increased in the order of chloride < nitrate < acetate precursor, was expected to have a significant influence on the reactivity [83]. The effect of metal loading on the product distribution was explained in a similar way. For 1% Rh/SiO_2 catalyst, the Rh species were surrounded by hydroxyl groups of the support. CO-saturated Rh species, which were derived from CO_2, reacted with surface OH groups to form fine Rh carbonyl clusters. This type of adsorbed CO was not hydrogenated further, resulting in desorption as molecular CO. On the other hand, 10% Rh/SiO_2 catalyst achieved higher surface coverage of Rh than 1% Rh/SiO_2. Therefore, too few surface hydroxyl groups existed around Rh particles, insufficient to form Rh carbonyl clusters. The coverage of hydride species on this Rh surface was higher than that of CO species, resulting in CH_4 formation [82].

The turnover frequency for CO_2 methanation on highly dispersed Rh/SiO_2 (514×10^{-5} s^{-1}) prepared by cation exchange was about fifty times higher than on a low dispersion Rh/SiO_2 (9.2×10^{-5} s^{-1}) and comparable to a high dispersion Rh/TiO_2 catalyst (803×10^{-5} s^{-1}) [84].

Rh/SiO_2 promoted with CeO_2 also showed high activity in CO_2 methanation [85]. This is probably cause by the presence of vacancies at the Rh and the reduced CeO_2 interface. High temperature reduction of Rh/CeO_2 and $Rh/CeO_2/SiO_2$ enhanced the catalytic activity in CO_2 methanation. The presence of oxygen vacancies in the bulk, formed in the large CeO_2 crystallites after reduction at 773 K, is believed to be the driving force leading to CO_2 activation [85]. The mechanisms of interaction between the ceria supported metals and CO_2 and the activation of CO_2 in the presence of H_2 to CH_4 are strongly influenced by the reduction temperature. It was suggested that by increasing the reduction temperature increased the reduction of bulk CeO_2, which is not promoted by the presence of metal [18]. It was suggested that the interaction mechanism involves the activation of CO_2 on surface Ce^{3+} sites with the formation of CO, followed by the oxidation of Ce^{3+} to Ce^{4+}. The presence of oxygen bulk vacancies will create the additional driving force for the reduction of the CO_2 to CO and/or surface carbonaceous species, which then rapidly hydrogenated to CH_4 over the supported metal [18].

Earlier, it was found that silica-supported Rh catalysts are efficient above 25 bar for C_2 oxygenate (ethanol, acetaldehyde, and acetic acid) production from CO + H_2 mixture [86,87] and so it would be expected that Rh/SiO_2 can convert CO_2 + H_2 into oxygenates while there are some proposed mechanisms that the reaction proceeds through CO intermediate. However, against expectations, 5% Rh/SiO_2 produces almost exclusively methane [60,65]. The addition of more than 30 metal oxide promoters to the catalysts was tested in the case of Rh/SiO_2. It was found that only four additives (Li, Fe, Sr, and Ag) showed ethanol formation [60]. On Rh-Li/SiO_2 (T = 513 K, P = 5 MPa), 15.5% ethanol selectivity at 7% CO_2 conversion was achieved and 43.1% methanol selectivity was found at 2.8% CO_2 conversion on the Rh-Sn/SiO_2 sample [60]. The addition of Fe influenced the CO_2 conversion as well as the ethanol selectivity reaching a maximum at a Fe/Rh atomic ratio = 2. It was 16% and the CO_2 conversion was 26.7% over 5% Rh-Fe(1:2)/SiO_2 catalyst at 5MPa and 533 K [88,89]. The effect of the Fe was interpreted as Fe influenced the electronic states of Rh. A good correlation was observed between the oxidation state of Fe and the product selectivity. It was suggested that Fe^0 promoted the methanation as well as the dissociation of adsorbed CO intermediate and the non-metallic Fe is responsible for the higher conversion and higher alcohol selectivity [88].

A comparative study of CO and CO_2 hydrogenation at 20 atm and 543 K shows that, although Rh and Rh-Fe/TiO_2 [90] and Rh-Fe/SiO_2 [87] catalysts exhibited appreciable selectivity to ethanol during CO hydrogenation, they functioned as a methanation catalyst during CO_2 hydrogenation, but ethanol (S_{EtOH}% = 6.4) and higher hydrocarbons (S_{C2+}% = 6.18) were also formed [90].

In the catalytic hydrogenation of CO_2 over Rh-Co/SiO_2 catalysts, the amount of cobalt added influenced the methanol selectivity as well as the CO_2 conversion. By means of XRD and XPS results, Rh-Co alloy formation was proposed; this process changes the electronic states of rhodium, resulting in the increase of methanol formation [91,92]. A good correlation was found between selectivity of methanol production and the surface composition of Rh-Co/SiO_2 catalysts determined by XPS. It was suggested that methanol formation was promoted on the interface between Rh and Co [92].

Lanthana addition to the Rh/SiO_2 increases the CO formation in the CO_2 + H_2 reaction, which does not react further to oxygenated products as in the CO hydrogenation [93].

When the Rh/SiO_2 was promoted with Ag the main product was CO but acetic acid formation was observed at 2 MPa pressure [94]. Its selectivity, taking into account hydrogenated products, was 61.3%. In CO hydrogenation Ag addition to Rh/SiO_2 suppressed the formation of C_2-oxygenates while in the CO_2 + H_2 reaction it remarkably promoted the CH_3COOH production. The possible pathway to acetic acid from CO_2 is the direct incorporation of CO_2; the reaction of adsorbed CO_2 with methyl groups to form acetic acid was suggested as a possibility [95]. Similar mechanism was described for acetic acid synthesis in the CH_4 + CO_2 step-wise reaction over Rh/SiO_2 catalyst [96].

5.3. Reaction of CO_2 with H_2 on Alumina Supported Rh Catalysts

The reaction of CO_2 + H_2 on Rh/Al_2O_3 produces almost exclusively methane [46,49,65,79,97]. From a comparison of the specific activities of Rh/Al_2O_3 in the H_2 + CO_2 and H_2 + CO reactions, it appears that the hydrogenation of CO_2 occurs much faster than that of CO [65]. It was found that the activity of Rh/Al_2O_3 to methane did not depend on the particle size at temperatures between 185 and 200 °C, whereas at lower temperature larger particles favored higher activity and on these species the activation energy was lower [79].

The CO and CO_2 hydrogenation was compared on Rh/Al_2O_3 using temperature programmed pulsed reaction experiments [98]. It was observed that the rate of hydrogenation of $C_{(ads)}$ from CO_2 was quicker than that of CO. This higher rate is probably due to easier availability of surface hydrogen because of reduced competition in the absence of adsorbed CO and less surface carbon [98].

The presence of oxygen could have a positive effect on the methanation of CO_2 [49]. When the oxygen concentration is higher than ~2%, it has a negative effect. DRIFT experiments explain that the positive effect of oxygen is due to the formation of more reactive species than the linearly bonded CO,

such as gem-dicarbonyl. On the contrary, the negative effect could be attributed to the oxidation of the catalyst [49].

On Rh/Al_2O_3, reversible structural changes were observed at atmospheric pressure and at relatively low temperatures (<350 °C) during the CO_2 methanation under transient operation conditions. Such changes were not observed for the Rh/SiO_2 catalyst, which also exhibits lower CO_2 conversion. Some of the Rh atoms are found to be in a low oxidation state (RhO_x) for the highly active Rh/Al_2O_3 during the CO_2 methanation. According to the in situ DRIFTS results, mainly linearly and bridge-bonded CO are formed on the Rh surface during CO_2 hydrogenation over both alumina and silica supported catalysts suggesting that a metallic Rh phase is required for the dissociation of CO_2. However, the oxygen resulting from the CO_2 dissociation reacts with some other Rh atoms and form RhO_x as revealed by XAS and XRD measurements. The linearly adsorbed CO species on metallic Rh are responsible for the higher activity of Rh/Al_2O_3. Thus, it is concluded that CO_2 methanation over Rh/Al_2O_3 proceeds by the dissociative adsorption of CO_2 giving rise to linearly adsorbed CO species on reduced Rh (Rh-CO_{lin}), whereas the adsorbed O can interact with other Rh atoms forming RhO_x [99].

The hydrogenation of CO_2 to methane was studied on Rh/Al_2O_3 doped with different metals (Cr, Fe, Co, Mo, P, Sn, and Pb). The additives lead to an increase in the binding energy of Rh 3 $d_{5/2}$ electrons and increase in the heat of hydrogen adsorption with the exception of Sn and Pb. The methanation rate has a maximum as a function of hydrogen adsorption heat [100].

The effect of Ba and K addition to Rh/Al_2O_3 catalysts in CO_2 hydrogenation reaction has been investigated by Büchel et al. [101]. Pure Rh/Al_2O_3 as well as the Ba-containing catalysts showed high CH_4 selectivity below 773 K with a maximum yield at 673 K, whereas, above this temperature, the reverse water gas shift reaction leading to CO and H_2 started to become dominant. In contrast, on K-containing catalysts CH_4 was not formed; all CO_2 was directly converted to CO in the whole temperature range of 573 to 1073 K. The effect of K was explained by the fact that due to the weak interaction between the catalysts and CO; CO was rapidly desorbed before being further reduced [101].

The hydrogenation of CO_2 on Rh/Al_2O_3 modified with Ni and K was also studied [41]. The catalytic tests show in these cases, too, that the K additive promotes the CO formation. On Rh/Al_2O_3, methane was the main product as found earlier [65,79,102], but the reaction was less selective to CH_4 on $Rh,K/Al_2O_3$ and on $Rh,Ni/Al_2O_3$; on $Rh,K,Ni/Al_2O_3$ CO, formation was preferred [41]. It was found that K changes the surroundings of Rh affecting the adsorption sites of CO and influences the activation ability for H_2 dissociation as well as the strength of CO adsorption.

Mechanical mixture of Rh/Al_2O_3 and Ni/AC (activated carbon) shows a significant catalytic synergy in the methanation of CO_2 [103]. This observation was explained by the cooperation between the two components. Rh/Al_2O_3 is highly efficient in CO_2 adsorption and Ni/AC is able to adsorb high quantities of H_2. It was supposed that the activated hydrogen migrates from Ni/AC towards Rh/Al_2O_3 and reacts with the adsorbed CO_2 [103].

Similar results were obtained when the reaction was studied on the mechanical mixture of Rh/Al_2O_3 and Pd/Al_2O_3 catalyst. It was found that although Pd/Al_2O_3 is inert under these conditions, the activity of the mechanical mixtures of the two catalysts was higher up to 50% than that of the pure Rh/Al_2O_3 [102]. The oxidation state of Rh or Pd in mono and bimetallic catalysts was nearly the same. No indication of segregation of one metal to the surface of the other was observed that can lead to the formation of bimetallic structures in the mixtures. From the kinetic data it was concluded that H_2 activated mainly over Rh/Al_2O_3, but the activation of CO_2, its dissociation to $CO_{(ads)}$ and subsequent hydrogenation to methane can take place on both catalysts [102].

5.4. Reaction of CO_2 with H_2 on Other Supported Rh Catalysts

The reaction was studied not only on the aforementioned carriers (TiO_2, Al_2O_3, and SiO_2), but many other oxides were also used as catalyst supports, such as CO_2 [15,18,47,73,85,104], Nb_2O_5 [61,63,64,67,73,105], MgO [65,67,68,98,106], ZrO_2 [61,67,68,107], etc.

Table 1. Comparison of the kinetic data for CO_2 + H_2 reaction obtained on different Rh catalysts.

	D%	Particle Size (nm)	E_a kJ/mol	x	y	Reference
5% Rh/SiO_2	22.8		72.4	0.64	0.27	[66]
3.4% Rh/SiO_2	45	2.2	69.5	0.53	−0.46	[39]
2.3% Rh/SiO_2	27		66.6	-	0.4	[68]
1.047% Rh/SiO_2			99.2	-	-	[84]
2.3% Rh/ZrO_2	51		62.4		0.4	[67,68]
5% Rh/Al_2O_3	30.2		67.8	0.61	0.26	[12,65]
1% Rh/Al_2O_3	30	3.6	95			[79]
2% Rh/Al_2O_3	18	6.1	66.1			[79]
3% Rh/Al_2O_3	7.1	15.4	61.1			[79]
2.3% Rh/Al_2O_3	6		71.2			[67,68]
1% Rh/TiO_2	22.3		81.1			[65]
1% Rh/TiO_2	7.8		103			[77]
1% Rh/TiO_2 + 2% WO_3	16.9		72.8			[77]
0.5% Rh/TiO_2			102.8 for CH_4 54.8 for CO	0 1	0.49 1.1	[78]
0.5% Rh/TiO_2 + 0.45% W^{6+}			69.4 for CH_4 26.3 for CO	0 1	0.53 0.95	[78]
0.5% Rh/TiO_2	61	2	120.2	0.83	−0.36	[69]
1% Rh/TiO_2	24	5	81.2	0.75	−0.15	[69]
3% Rh/TiO_2	6	17	71.2	0.58	0.01	[69]
5% Rh/TiO_2	6	19	68.2			[69]
2.3% Rh/MgO	27		96.7			[67,68]
0.67% Rh/MgO	29		92			[106]
2.3% Rh/Nb_2O_5	6		69.9			[67]
Rh foil			71.2	0.5	0.2	[54]
Rh foil			67	-	-	[25]
Rh foil			75			[57]

E_a apparent activation energy, x and y the partial order of H_2 and CO_2, respectively.

The role of the ceria based catalysts in the hydrogenation of CO_2 is summarized recently [108]. These samples have been found to have higher activity and selectivity to methane with respect to many other oxides [15,47,73]. This behavior was attributed to the presence of oxygen vacancies on the reduced ceria. It was suggested that by increasing the reduction temperature a progressive reduction of the bulk CeO_2 takes places which is not promoted by the metal. Please note, however, that others found that Rh promotes the reduction of the CeO_2 surface [109]. The oxygen vacancies which are formed in the large CeO_2 crystallites after reduction at 773 K but not after low temperature reduction are the driving force for CO_2 activation with the formation of CO and the oxidation of reduced ceria. The role of the supported metal is providing the active H species for hydrogenation [18,85].

Different in situ measurements (AP-XPS, HE-XRD, and DRIFT) revealed that the Ce^{3+} species are likely the active sites in CO_2 methanation for ceria-based catalysts [104].

The hydrogenation of CO_2 was investigated over Rh catalyst prepared from amorphous $Rh_{20}Zr_{80}$ alloy and the results were compared with Rh/ZrO_2 prepared by conventional impregnation method. It was found that the CH_4 formation rate related to surface Rh was slightly higher for the alloy precursor catalyst [110]. When the reduction temperature was raised, the CH_4 selectivity decreased above 620 K for the impregnated Rh/ZrO_2 and above 720 K for the alloy precursor catalyst [110]. The activities of Rh/ZrO_2 prepared by different methods were compared [111]. The product was mainly CH_4 but on the impregnated sample CO was formed. The highest CO_2 conversion was found on the

sample prepared by the water-in-oil microemulsion method. The higher activity of this sample may be attributed to the small Rh particle size, the location of the Rh particles and the interaction of Rh and the carrier [111]. The effect of promoter (Li, K, Ce, Re, and Co) was studied in the case of Rh-Mo/ZrO_2 catalysts during CO and CO_2 hydrogenation. In the CO + H_2 reaction, at 15 atm pressure, a significant amount of methanol was formed (selectivities were 22.7–33.2%), whereas in CO_2 hydrogenation under the same experimental conditions, lower conversions were observed in all cases and only methane was produced. When the CO hydrogenation was studied in the presence of CO_2, the turnover number for methanol formation decreased indicating that CO_2 may partially blocked the sites required for the CO hydrogenation [107]. On Rh/ZrO_2 at atmospheric pressure in the CO_2 + H_2 reaction the CO_2 conversion (23% at 453 K) was more than 20 times higher than the CO conversion in CO hydrogenation (1% at 453 K) [68].

Rh/Nb_2O_5 catalyst gives C_{2+} hydrocarbons consisting mainly of C_2H_6 and C_3H_8 with 30–50% selectivity at temperatures ranging from 250 to 350 °C even at atmospheric pressure [63]. The conversion of CO_2 on this catalyst was significantly lower (4% at 523 K) than on Rh/TiO_2 (29%) or $RhZrO_2$ (8%), but on the former sample, only CH_4 was produced, whereas on the latter catalyst, the selectivity for C_2+ hydrocarbons was significantly lower [63]. It was found that the C_{2+} hydrocarbon formation was influenced by the structure of the Nb_2O_5 support [105] and the selectivity increased with increasing the reduction temperature [64,105]. Comparing the activity of different supported Rh catalysts in the CO and CO_2 hydrogenation only on Rb/Nb_2O_5 was found higher activity for CO conversion than that of CO_2 [67]. When the pressure was increased to 10 bar methanol was formed on Rh/Nb_2O_5 catalyst [61]. The selectivity of it drastically decreased as the temperature increased. The selectivity was lower than on Rh/TiO_2 but the rate of methanol formation was higher (100 μmol h^{-1} g-catal^{-1}).

Rh/MgO is not one of the most active catalysts [65,67,68]; in this case, different results were obtained by different research groups. Some have reported that Rh/MgO activity decreases continuously in time and does not reach steady state [65]. The reaction product was almost exclusively CH_4 below and at 473 K [67,106], but above 523 K, CO was the main product [67]. The apparent activation energies of CO_2 and CO hydrogenation to form CH_4 at the steady-state reaction were nearly the same, 92 kJ/mol, however the rate of CO_2 conversion was eight times higher than that of CO. These observations strongly suggested that common intermediates form CH_4 with the same kinetic structure in both reactions. In CO hydrogenation an appreciable amount of adsorbed CO is accumulated on the surface during the reaction inhibiting the reaction of the intermediates with H_2 and this resulted in the higher rate for CO_2 hydrogenation [106].

When Rh was supported on La_2O_3 in the CO_2 hydrogenation mainly CO was formed (S_{CO}% = 82.5% at 513 K) and the conversion was much higher (30.3% at 513 K) than in the CO + H_2 reaction (5.6%), but in the latter case, besides methane and CO_2, C_{2+} hydrocarbons, methanol, ethanol, and acetic acid (S_{ox}% = 39.3% at 513 K) were also formed [93].

Rh-doped $SrTiO_3$ synthetized by hydrothermal methods shows better activity, higher yield, and selectivity for CO formation in the CO_2 + H_2 reaction than the conventional Rh/$SrTiO_3$ catalyst. The excellent activity is attributed to the cooperative effect between the sub-nanometer Rh clusters, which are effective in the dissociation of H_2 and the reconstructed $SrTiO_3$ with oxygen vacancies for preferential adsorption/activation of CO_2 [112].

Rh ion-exchanged Y-type zeolite showed 10 times higher activity in the CO_2 hydrogenation (H_2/CO_2 = 3, total pressure 3 MPa, 423 K) than a conventional impregnated Rh/SiO_2 [113].

Significant amount of methanol formation was detected in the reaction, but after 100 min serious deactivation was observed; it was attributed to the deposition of water inside the zeolite cage. The active Rh sites were determined as Rh particles (2–3 nm) located outside of the cage. It was supposed that the zeolite cage played a role to condense CO_2 and to supply to Rh sites outside the cage [113].

The catalytic selectivity is strongly related to the environment of the Rh nanoparticles. Pure silica MFI-fixed Rh nanoparticles exhibited maximized CO selectivity at high CO_2 conversion, whereas aluminiumsilicate MFI zeolite (ZSM-5)-supported Rh nanoparticles displayed high CH_4 selectivity

under equivalent conditions. When K ions were introduced by ion exchange into the HZSM-5 preparing Rh/KZSM-5catalyst, the CO selectivity markedly enhanced; the CO selectivity strongly depended on the amount of K^+ in the catalyst. It was concluded when the hydrogen spill over is hindered then the CO formation is favorable, and the significant spill over should be attributed to the abundant acidic sites of Rh/ZSM-5 [114].

The CO_2 hydrogenation was performed over Li promoted Rh ion-exchanged zeolite catalysts at 3 MPa pressure [72,115]. As the amount of added Li increased, the selectivity of methane formation decreased and CO was formed. When the Li/Rh ratio was 10 the selectivity for CO reached 87% and alcohol formation was also observed, the methanol and ethanol selectivity was 2.3% and 2.7%, respectively.

6. Surface Species Formed in the Interaction and in the Reaction of CO_2 with H_2 on Supported Rh

To understand the mechanism of a reaction, it is necessary to investigate the interaction of the reaction partners on the surface of the catalysts, to identify the species formed and exist on the reaction surface during the reaction and to determine their reactivity.

The adsorption measurements revealed that, with the exception of Rh/SiO_2, the presence of H_2 greatly enhances the uptake of CO_2 by Rh supported on different oxides (TiO_2, Al_2O_3, and MgO) [37,48].

Infrared spectroscopic measurements show that besides different carbonates, formate groups (except for SiO_2 supported sample) and CO are formed in the low temperature interaction [37,41,48] and during the CO_2 hydrogenation. Comparing the IR spectra of adsorbed CO_2 and formic acid on clean supports, similar spectra were registered as on the supported Rh samples. It means that the carbonates and the formate are located not on the Rh but rather on the supports. In this case, the only interesting question may be why the absorption bands of one form or the other are missing from the spectrum. The amount and the nature of the adsorbed species are dependent on the annealing temperature of the support, on the nature of the surface OH groups, i.e., on the basicity of the surface [116]. For example, on γ-Al_2O_3 annealed at 473 K, mostly bicarbonates formed, whereas no adsorbed CO_2 was detected on this highly hydroxylated surface. With increasing calcination temperature the surface concentration of carbonates and linearly adsorbed CO_2 increased but bicarbonates remained the most abundant surface species [117]. When the Rh/Al_2O_3 was promoted with K it was assumed that no potassium formates were formed, but rather formates that were adsorbed at the alumina surface in the vicinity of K [41]. Some groups suggested that carbonates and formates are only spectator molecules, whereas, in the opinion of others, these surface species, despite the location of their adsorption centers, are actively involved in the CO_2 + H_2 reaction. The formate species formed after the adsorption of HCOOH at room temperature on Rh/Al_2O_3 at 423 K decomposed to CO_2 and H_2 (~70%) and to CO and H_2O (~30%), CH_4 was formed only in traces. When the formate ion was treated with H_2 at the same temperature, 70% of the adsorbed species was converted to CH_4 [118]. Similar results were found on lanthanide-oxide promoted Rh/Al_2O_3 [119]. The admission of H_2 onto preadsorbed CO_2 on Rh/MgO results in a decrease of the 1650 cm^{-1} band due to the hydrogen carbonate band and at the same time in the appearance of formate band at 1600 cm^{-1} [37]. These observations clearly show that the hydrogen carbonate could be converted to formate and the formate to CH_4.

Before examining the spectra of adsorbed CO formed in the reaction or in the interaction, let us examine first the forms in which the CO gas is adsorbed. The linearly bonded CO (Rh-CO) absorbs at 2040–2075 cm^{-1} depending on the coverage, the characteristic bands for the twin or dicarbonyl ($Rh(CO)_2$) structure are at ~2100 and ~2030 cm^{-1}, and the peak due to the bridge bonded form Rh_2CO can be detected at 1830–1850 cm^{-1}. The $Rh_2(CO)_3$ form absorbs at 1905–1925 cm^{-1}. There are some minor species bonded to the oxidized Rh surface [120,121].

The spectral feature of CO formed in the co-adsorption or in the reaction of CO_2 + H_2 differed basically from that observed during the adsorption of gaseous CO. The IR spectra of adsorbed CO on different supported Rh have been the subject of several papers; the doublet due to the twin structure ($Rh(CO)_2$) was missing and the linearly bonded CO absorbed at lower frequencies (~2030–2020 cm^{-1}).

It was suggested that the adsorbed hydrogen prevents the formation of the twin structure and Rh carbonyl hydride was formed [37,41,42,48,122].

The chemisorbed H is electron donating, the π back-donation from Rh into the antibonding orbital of CO increases, and thus the carbonyl band appears at lower frequencies [37,41,48]. Iizuka and Tanaka [68,123] stated that the bands observed in the 2020–2040 cm^{-1} region on the infrared spectra, over supported Rh were due to a linear CO species at low coverage rather than to a carbonyl hydride. Henderson and Worley using D_2, instead of H_2, confirmed the Rh carbonyl hydride formation [122]. The absorption frequency of linearly bonded CO formed in the reaction depends on the Rh dispersion, i.e., on the Rh particle size. Catalysts with low Rh dispersion have a higher frequency of absorption compared with the catalysts with higher Rh dispersion [79].

When 10% Rh/SiO_2 was reduced and cooled down in hydrogen after CO_2 adsorption linear CO was observed at 2029 cm^{-1}. Upon H_2 introduction the peak moved to higher frequency and a broad band at 1795 cm^{-1} was also found. This was also observed during CO_2 hydrogenation. The frequency of this band red-shifted to 1749 cm^{-1} as the temperature increased. This absorption was attributed to the formation of hydroxicarbonyl species [82].

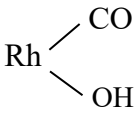

When Rh/Al_2O_3 was not reduced before the reaction the structure of the adsorbed CO changed during the reaction due to the progressing reduction of Rh^+ and agglomeration effects. First at 523 K geminal dicarbonyl species are present, Rh^0-CO are observable at 573 K and then the band around 2020 cm^{-1} becomes dominant [41].

On lanthanide-promoted Rh/Al_2O_3, two peaks were observed in the CO region at ~2050 and ~2030 cm^{-1} in the $CO_2 + H_2$ reaction, but only one peak was detected at 2023 cm^{-1} on the unpromoted catalyst [124]. The band at ~2020 cm^{-1} was assigned to adsorbed CO on Rh(I) sites.

The formation and adsorption of CO from $CO_2 + H_2$ occurs according to high pressure FTIR measurements on Rh/Al_2O_3. The main CO species, hydride CO, increase with increasing the CO_2 pressure. In the presence of water vapor the absorption band of hydride CO is shifted to the lower frequency range of 2000 to 1880 cm^{-1}; such a significant change was not observed for the bridged CO absorption at 1880–1740 cm^{-1} [125]. The direct interaction between the CO and the water was excluded, the shift was explained that the CO was displaced preferentially by water from atomically rough surface.

On Rh/TiO_2 [42], formyl groups were also found absorbing at 1720 cm^{-1}. The intensity of this band shows a maximum as a function of reduction temperature. These results could be explained by the observation that the interfacial sites in TiO_x/Pt promote the decomposition of CH_xO intermediates [126]. As the higher reduction temperature increases both the formation and the decomposition rate of formyl groups the resultant is the maximum in the surface concentration.

On Fe-promoted 5% Rh/SiO_2 catalysts (Fe/Rh = 0–0.5), in the $CO_2 + H_2$ reaction, as was mentioned earlier, ethanol was also formed. Infrared spectroscopic measurements revealed that adsorbed CO species were observed on each catalyst. Linear CO species at 2020–2050 cm^{-1} shifted to higher wave number with an added amount of Fe in the range of Fe/Rh = 0–0.1. The shift corresponds to a decrease in reverse donation from Rh to adsorbed CO and an increase in the C–O bond strength. In contrast the linear species shifted to lower wave number again with added Fe in the rage Fe/Rh = 0.3–0.5. The Fe

additives influenced not only the linear but the bridge bonded CO, too. The ratio of the bridge and linearly bonded CO increased with increasing the amount of Fe. By comparing this ratio with the ethanol selectivity, it was concluded that the ethanol selectivity correlates with the intensity of the bridged CO [88].

In situ ED-XAS and HE-XRD studies demonstrated that on Rh/Al_2O_3 the Rh is not in a pure metallic state; it was in a low oxidation state (RhO_x) during the methanation reaction. This is a strong indication that CO_2 dissociates forming adsorbed CO and O [99]. Such changes were not observed for the Rh/SiO_2 catalyst, which exhibits lower CO_2 conversion. In situ DRIFTS results indicated that mainly the linearly (~2020 cm^{-1}) and bridge bonded CO (1780 cm^{-1}) were formed during the CO_2 hydrogenation over both Al_2O_3 and SiO_2 supported samples, but the intensity of the Rh-CO species band was much stronger on Rh/Al_2O_3 than on Rh/SiO_2. It was also accepted that the shift in the CO absorption frequency is due to the Rh-carbonyl-hydride formation [99].

On 1% Rh/Al_2O_3, under reaction conditions at 323 K, the CO band appeared at 2036 cm^{-1} (Rh^0-CO). When the temperature increased the band intensities increased and at the same time they shifted to lower wave numbers reaching 2021 cm^{-1} at 473 K [79]. At this temperature, a broad band at 1805 cm^{-1} attributed to bridge-bonded CO ($Rh^0{}_2CO$) was also detected. On catalysts containing 2% or more Rh supported on Al_2O_3 a weak band was also observed at 1905 cm^{-1}, which was related to the formation of $Rh_2(CO)_3$ [79]. On potassium promoted Rh/Al_2O_3 the intensity of the linearly bonded CO was negligible and an additional band was observed at 1794 cm^{-1} at 623 K. This band is only observable under reaction conditions and vanishes during flushing with He and it was attributed to adsorbed formyl (HCO) species [41].

During the CO_2 + H_2 reaction on Rh/TiNT and on Rh/TiNW, peaks were registered in the CO region not only at 2030–2050 cm^{-1}, but at 1760–1770 cm^{-1}, too. This feature was assigned to such type of tilted CO which bonded to the Rh and interacts with the oxygen vacancy of the titanate support. This suggestion was based on the earlier observations that Lewis acid sites interact with the oxygen atom of CO which resulted in a downward shift of the CO absorption wave number [127,128]. The other possible assignation of this peak would be the C=O band in the adsorbed HCHO. This was ruled out because this species on Rh/TiO_2 absorbs at 1727 cm^{-1} [129].

7. The Proposed Mechanism for the CO_2 Hydrogenation on Supported Rh Catalysts

Regarding the reaction mechanism for CO_2 hydrogenation basically two different, but same in a few steps reaction mechanisms were proposed. The first involves the adsorption of CO_2 on the support and its reaction with $H_{(ads)}$ formed on the metal, which leads to the formation of formate (HCOO) or formyl (HCO) at the metal support interface [39,54,104]. The second mechanism involves the direct or hydrogen assisted dissociation of CO_2 on the metal surface and the subsequent hydrogenation of adsorbed CO through surface carbon forming CH_x and then CH_4 [45,65]. There is a general agreement in this case that the dissociation of the adsorbed CO is the rate determining step. Many variations of both main directions have been described. Still, there is discussion on the nature of the intermediate compounds involved in the reaction process and on the products formation scheme. It is not so easy to distinguish between the real reaction intermediate and the spectator molecules, whereas, in most publications, the same surface species were found. Support dependent reaction mechanisms were suggested for CO_2 hydrogenation via either a CO route for catalyst supported on non-reducible support [99] or the formate route for catalysts supported on reducible oxides [104,130,131]. Others suggested that oxygen vacancies play an important and major role in the dissociation of CO_2 in the case of reducible oxide supported catalysts [59,85]. It was assumed that the CO evolved in the CO_2 dissociation reacts further by the same mechanism as in the CO + H_2 reaction.

If the adsorbed CO species play an important role in the hydrogenation of CO_2, the question arises as to why the formation of CH_4 is faster in the CO_2 + H_2 reaction than when the H_2 + CO mixture was used. There is an assumption that CO adsorbs on the metal sites thus reducing the possibility of hydrogen dissociation [72]. It was supported by the finding that the partial order of CO at

relatively high CO concentration (33%) was negative [132]. It is another suggestion [11,45,65] whether the surface concentrations of adsorbed CO and the surface C play the key roles. When CO_2 was used, the concentration of adsorbed CO, and therefore the concentration of surface carbon produced in the direct or in the hydrogen induced dissociation of CO, was relatively low. The carbon formed can react quickly with the large excess of H_2, and there is less possibility for the accumulation and aging of surface C. In contrast, when a H_2 + CO gas mixture was used, the surface concentration of adsorbed CO is higher and so the formation of surface carbon will be much larger during a given time. Consequently, not all the surface carbon reacts immediately with hydrogen and a part of the surface carbon transformed to less reactive forms [C_x]. The hydrogenation rate of this species is slower and requires probably higher activation energy. The aging of carbon is well demonstrated by the study of the reaction of carbon deposit (formed in the H_2 + CO_2 or in the H_2 + CO reaction [133] or in CO disproportionation [132]) with H_2 on different supported Rh catalysts. The reactivity of the surface carbon formed in the dissociation or in the disproportionation of CO depended on the temperature of its formation and also on the time between its formation and its coming into contact with H_2 [132]. On the other hand, when a H_2 + CO mixture was used, CO adsorbed on Rh can function as a poison toward hydrogen chemisorption, therefore resulting in a decreased methanation rate, and the surface carbon has time to age.

In the previous chapter we have shown that different adsorbed CO species were detected during the reaction. There is even no consent in which detected CO form is actually involved in the hydrogenation of CO_2. There are groups that have suggested that linearly bonded CO [54,72] or the carbonyl-hydride form [65] is the most important surface intermediate, while others have proposed the bridge bonded CO [60,88] but there is also example that the dicarbonyl structure reacts further to methane [49]. There is another assumption that the intermediate species in the CO_2 hydrogenation on Rh/MgO, Rh/Al_2O_3, and Rh/CeO_2 is the $[M_y]Rh_xH_n(CO)_p$ (M = Mg, Al, Ce) complex [47].

In the following, some specific examples are presented in which the mechanism of the CO_2 + H_2 reaction is described in different ways.

The methanation of CO_2 on titania deposited Rh foils [51] and Rh/SiO_2 [39] is proposed to start with the dissociation of CO_2 into $CO_{(a)}$ and $O_{(a)}$ and then proceeds through steps which are identical to those for CO hydrogenation.

$$CO_{2(g)} + 2S \rightleftharpoons CO_{(a)} + O_{(a)} \quad (1)$$

$$H_{2(g)} + 2S \rightleftharpoons 2H_{(a)} \quad (2)$$

$$2H_{(a)} + CO_{(a)} \rightleftharpoons H_2CO_{(a)} + 2S \quad (3)$$

$$H_2CO_{(a)} + S \rightarrow CH_{2(a)} + O_{(a)} \quad (4)$$

$$O_{(a)} + H_{(a)} \rightleftharpoons OH_{(a)} + S \quad (5)$$

$$CH_{2(a)} + H_{(a)} \rightleftharpoons CH_{3(a)} + S \quad (6)$$

$$CH_{3(a)} + H_{(a)} \rightleftharpoons CH_{4(g)} + 2S \quad (7)$$

It was assumed that the rate limiting step is the dissociation H_2.

$$CH_{4(ads)} \rightarrow C_{(ads)} + 4H_{(ads)} \quad (8)$$

$$CO_{2(ads)} \rightarrow CO + O_{(ads)} \quad (9)$$

Kusama et al. [83] proposed that the first step of CO_2 hydrogenation on Rh/SiO_2 is the reaction of CO_2 with H_2 and the formation of adsorbed CO on Rh surface. CO saturated Rh surface species react with the surface hydroxyl groups and form Rh-carbonyl clusters

$$[Rh]_n + 2CO + xHO\text{-}Si\ [Rh]_{n-1}{+}Rh(CO)_2(O\text{-}Si)_x + x/2H_2 \quad (10)$$

Adsorbed CO was not subjected to further hydrogenation and just desorbed as CO. With this theory, the high CO selectivity on Rh/SiO_2 could be explained.

Earlier, it was suggested that the CO in Rh carbonyl hydride dissociates to surface carbon which reacts further to methane, but the carbon lost its activity in time [65].

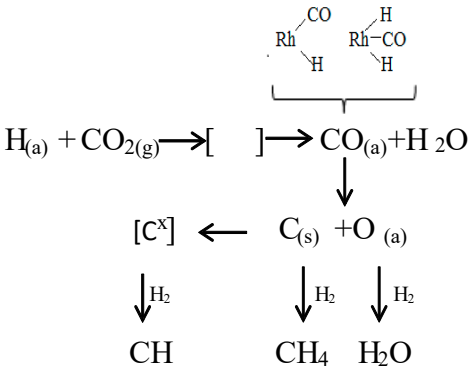

Similar reaction scheme was suggested for CO_2 hydrogenation on Rh/TiO_2 catalyst [45].

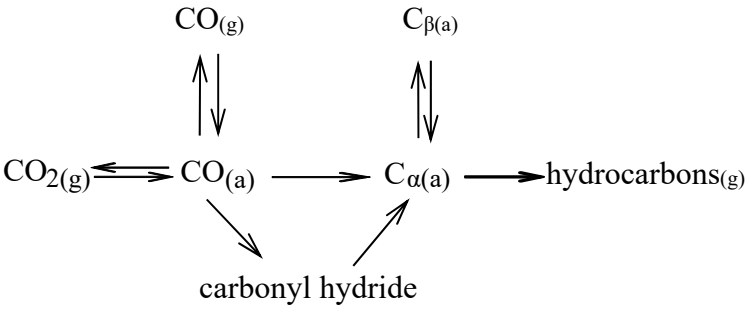

It was supposed based on the results of ambient-pressure XPS, DRIFT, and high-energy XRD measurements that the ceria phase is partially reduced during the CO_2 methanation on Rh/CeO_2, and, in particular, Ce^{3+} species seem to facilitate the activation of CO_2 molecules. The activated CO_2 species then react with hydrogen atom produced from H_2 dissociation on Rh sites and formate species are formed. The higher methane selectivity on Rh/CeO_2 is explained by the stronger metal–support interaction [104].

Several works proposed that CO dissociation is assisted by hydrogen and carbonyl-hydride can be formed which weakens the C–O bond related to that in carbonyl [65].

This suggestion is supported by the CO spectra registered during the reaction, while the CO band appeared at lower wave number than after CO adsorption. Although this is a significant evidence for the hydrogen assisted C–O bond cleavage, but there is no direct evidence for the existence of H_nCO surface species during the hydrogenation of CO_2.

On Li promoted Rh/SiO_2 ethanol formed in the $CO_2 + H_2$ reaction but on Rh/SiO_2 the methane selectivity was 99.7%. The effect of Li in the ethanol formation was explained with the difference observed in the adsorbed CO formed during the reaction. On the IR spectra of $Rh\text{-}Li/SiO_2$, the intensity of bridge bonded CO was higher than that of the linear one, while on the undoped sample the intensities were the same. The more bridged CO (which occupies 2 Rh atoms) provide smaller number of unoccupied Rh sites for H_2 adsorption and thus the hydrogenation ability of the catalyst will be suppressed. Therefore, the CO species can be inserted into a CH_3-Rh bond more easily than on Rh/SiO_2 [60]. In the case of $Rh\text{-}Fe/TiO_2$, the ethanol production was also assumed through the formation of CH_3CO^* (acyl) groups [90].

The formation of acetic acid on Ag promoted Rh/SiO_2 was explained with the direct insertion of CO_2 to surface methyl species on Rh which led to acetate formation, followed by hydrogenation to acetic acid. Acetic acid formation suppresses remarkably the CO_2 dissociation and desorption over highly dispersed Rh catalyst at lower reaction temperature [94].

The adsorbed CO could be detected already at temperatures as low at which the gas phase products CO or CH_4 are not formed yet on Rh/TiO_2 [69], or on Rh/Al_2O_3 [48]. Some authors proposed a mechanism for $CO_{(ads)}$ production through the formation of formate species.

$$CO_2 + H_{(metal)} \rightarrow COOH_{(interface)} \rightarrow CO_{(metal)} + OH_{(support)} \quad (11)$$

Others suggested the direct dissociation of CO_2 on Rh in the interaction of $CO_2 + H_2$ [28]. It was assumed that the formates are mainly spectators and form in the reaction of $CO_{(ads)}$ with the OH groups of the support [69]

$$CO_{(metal)} + OH_{(support)} \rightleftharpoons COOH_{(interface)} \quad (12)$$

As we have seen in recent years, many ideas have been developed for the hydrogenation of CO_2, but, to date, there is no clear explanation as to what and why influences the activity and selectivity of Rh catalysts.

8. Conclusions

This review summarizes the studies on the hydrogenation of CO_2 on supported Rh catalysts. Comparing the activity and selectivity of different supported metal catalysts, it was found that Rh is one of the best samples. The possibility of the CO_2 dissociation on clean metal and on supported Rh was discussed separately. The results are not clear there are groups who have detected the dissociation of CO_2 while others have not observed this process. The hydrogenation of CO_2 produces mainly CH_4 and CO, but the selectivity of the reaction is affected by the support, in some cases the reduction of the support; the particle size of Rh; and the different additives. At higher pressure methanol, ethanol and acetic acid could be also formed. The activity of the various supported Rh catalysts was compared and in general, the TiO_2 and CeO_2 supported samples were the best. Results obtained for TiO_2-, SiO_2-, and Al_2O_3-supported catalysts were discussed in a separate chapter. The compounds formed on the surface of the catalysts during the reaction are shown in detail; mostly different CO species, adsorbed formate groups, and different carbonates were detected. In a separate chapter, the mechanism of the reaction was also discussed. Basically, two different, but similar in a few steps, reaction mechanisms were proposed. The first involves the adsorption of CO_2 on the support and its reaction with $H_{(ads)}$ which leads to the formation of formate (HCOO) or formyl (HCO). The other involves the direct or hydrogen assisted dissociation of CO_2 on the Rh surface and the subsequent hydrogenation of adsorbed CO through surface carbon-forming CH_x and then CH_4.

Conflicts of Interest: The authors declare no conflict of interest.

References

1. Earth System Research Laboratory Global Monitoring Division. Available online: https://www.esrl.noaa.gov/gmd/ccgg/aggi.html (accessed on 7 January 2020).
2. CO_2 Earth. Available online: https://www.co2.earth/daily-co2 (accessed on 7 January 2020).
3. Sabatier, P.; Senderens, J.-B. Hydrogénation directe des oxydes du carbone en présence de divers méltaux divisés. *Comptes Rendus* **1902**, *134*, 689–691.
4. Mills, G.A.; Steffgen, F.W. Catalytic Methanation. *Catal. Rev.* **1974**, *8*, 159–210. [CrossRef]
5. Wang, W.; Wang, S.; Ma, X.; Gong, J. Recent advances in catalytic hydrogenation of carbon dioxide. *Chem. Soc. Rev.* **2011**, *40*, 3703. [CrossRef]

6. Rönsch, S.; Schneider, J.; Matthischke, S.; Schluter, M.; Götz, M.; Lefebvre, J.; Prabhakaran, P.; Bajohr, S. Review on methanation–From fundamentals to current projects. *Fuel* **2016**, *166*, 276–296. [CrossRef]
7. Fechete, I.; Védrine, J.C. Nanoporous Materials as New Engineered Catalysts for the Synthesis of Green Fuels. *Molecules* **2015**, *20*, 5638–5666. [CrossRef]
8. Solis-Garcia, A.; Fierro-Gonzalez, J.C. Mechanistic Insights into the CO_2 Methanation Catalyzed by Supported Metals: A Review. *J. Nanosci. Nanotechnol.* **2019**, *19*, 3110–3123. [CrossRef]
9. Aziz, M.A.A.; Jalil, A.A.; Triwahyono, S.; Ahmad, A. CO_2 methanation over heterogeneous catalysts: Recent progress and future prospects. *Green Chem.* **2015**, *17*, 2647–2663. [CrossRef]
10. Younas, M.; Kong, L.L.; Bashir, M.J.K.; Nadeem, H.; Shehzad, A.; Sethupathi, S. Recent Advancements, Fundamental Challenges, and Opportunities in Catalytic Methanation of CO_2. *Energy Fuels* **2016**, *30*, 8815–8831. [CrossRef]
11. Aziz, M.A.A.; Jalil, A.A.; Triwahyono, S.; Sidik, S.M. Methanation of carbon dioxide on metal-promoted mesostructured silica nanoparticles. *Appl. Catal. A Gen.* **2014**, *486*, 115–122. [CrossRef]
12. Solymosi, F.; Erdőhelyi, A. Hydrogenation of CO_2 to CH_4 over alumina-supported noble metals. *J. Mol. Catal.* **1980**, *8*, 471–474. [CrossRef]
13. Panagiotopoulou, P. Hydrogenation of CO_2 over supported noble metal catalysts. *Appl. Catal. A Gen.* **2017**, *542*, 63–70. [CrossRef]
14. Panagiotopoulou, P.; Kondarides, D.I.; Verykios, X.E. Selective methanation of CO over supported noble metal catalysts: Effects of the nature of the metallic phase on catalytic performance. *Appl. Catal. A Gen.* **2008**, *344*, 45–54. [CrossRef]
15. Martin, N.M.; Velin, P.; Skoglundh, M.; Bauer, M.; Carlsson, P.-A. Catalytic hydrogenation of CO_2 to methane over supported Pd, Rh and Ni catalysts. *Catal. Sci. Technol.* **2017**, *7*, 1086–1094.
16. Muhammad, Y.; Sethupathi, S.; Kong, L.L.; Mohamed, A.R. CO_2 methanation over Ni and Rh based catalysts: Process optimization at moderate temperature. *Int. J. Energy Res.* **2018**, *42*, 3289–3302.
17. Wambach, J.; Baiker, A.; Wokaun, A. CO_2 hydrogenation over metal/zirconia catalysts. *Phys. Chem. Chem. Phys.* **1999**, *1*, 5071–5080. [CrossRef]
18. De Leitenburg, C.; Trovarelli, A.; Kašpar, J. A Temperature-Programmed and Transient Kinetic Study of CO_2 Activation and Methanation over CeO_2 Supported Noble Metals. *J. Catal.* **1997**, *166*, 98–107. [CrossRef]
19. Yaccato, K.; Carhart, R.; Hagemeyer, A.; Lesik, A.; Strasser, P.; Volpe, A.F., Jr.; Turner, A.F.; Weinberg, H.; Grasselli, R.K.; Brooks, C. Competitive CO and CO_2 methanation over supported noble metal catalysts in high throughput scanning mass spectrometer. *Appl. Catal. A Gen.* **2005**, *296*, 30–48. [CrossRef]
20. Solymosi, F. The bonding, structure and reactions of CO_2 adsorbed on clean and promoted metal surfaces. *J. Mol. Catal.* **1991**, *65*, 337–358. [CrossRef]
21. Freund, H.-J.; Roberts, M.W. Surface chemistry of carbon dioxide. *Surf. Sci. Rep.* **1996**, *25*, 225–273. [CrossRef]
22. Collins, A.C.; Trapnell, B.M.W. CO_2 chemisorption on evaporated metal films. *Trans. Faraday Soc.* **1957**, *53*, 1476. [CrossRef]
23. Campbell, C.T.; White, J.M. The adsorption, desorption, and reactions of CO and O2 on Rh. *J. Catal.* **1978**, *54*, 289–302. [CrossRef]
24. Yang, C.; Garland, C.W. Infrared Studies of Carbon Monoxide Chemisorbed on Rhodium. *J. Phys. Chem.* **1957**, *61*, 1504–1512. [CrossRef]
25. Sexton, B.; Somorjai, G.A. The hydrogenation of CO and CO_2 over polycrystalline rhodium: Correlation of surface composition, kinetics and product distributions. *J. Catal.* **1977**, *46*, 167–189. [CrossRef]
26. Dubois, L.; Somorjai, G.A. The dissociative chemisorption of carbon dioxide on rhodium surfaces. *Surf. Sci.* **1979**, *88*, L13–L17. [CrossRef]
27. Dubois, L.H.; Somorjai, G.A. The chemisorption of CO and CO_2 on Rh(111) studied by high resolution electron energy loss spectroscopy. *Surf. Sci.* **1980**, *91*, 514–532. [CrossRef]
28. Weinberg, W.H. Why CO_2 does not disWhy CO_2 does not dissociate on Rh at low temperature. *Surf. Sci.* **1983**, *128*, L224–L230. [CrossRef]
29. Goodman, D.W.; Peebles, D.E.; White, J.M. CO_2 dissociation on rhodium: Measurement of the specific rates on Rh(111). *Surf. Sci.* **1984**, *140*, L239–L243. [CrossRef]
30. Solymosi, F.; Kiss, J. Impurity effects in the adsorption and dissociation of CO_2 on Rh. *Surf. Sci.* **1985**, *149*, 17–32. [CrossRef]

31. Solymosi, F.; Kiss, J. The effect of boron impurity on the adsorption and dissociation of CO_2 on Rh surfaces. *Chem. Phys. Lett.* **1984**, *110*, 639–642. [CrossRef]
32. Kiss, J.; Révész, K.; Solymosi, F. Photoelectron spectroscopic studies of the adsorption of CO_2 on potassium-promoted Rh(111) surface. *Surf. Sci.* **1988**, *207*, 36–54. [CrossRef]
33. Solymosi, F.; Bugyi, L. Adsorption and dissociation of CO_2 on a potassium-promoted Rh(111) surface. *J. Chem. Soc. Faraday Trans. 1 Phys. Chem. Condens. Phases* **1987**, *83*, 2015–2033. [CrossRef]
34. Hendrickx, H.A.C.M.; Jongenelis, A.P.J.M.; Nieuwenhuys, B.E. Adsorption and dissociation of carbon dioxide on rhodium surfaces. *Surf. Sci.* **1985**, *154*, 503–523.
35. Van Tol, M.F.H.; Gielbert, A.; Nieuwenhuys, B.E. The adsorption and dissociation of CO_2 on Rh. *Appl. Surf. Sci.* **1993**, *67*, 166–178. [CrossRef]
36. Lambeets, S.V.; Barroo, C.; Owczarek, S.; Jacobs, L.; Genty, E.; Gilis, N.; Kruse, N.; De Bocarmé, T.V. Adsorption and Hydrogenation of CO_2 on Rh Nanosized Crystals: Demonstration of the Role of Interfacet Oxygen Spillover and Comparative Studies with O2, N2O, and CO. *J. Phys. Chem. C* **2017**, *121*, 16238–16249. [CrossRef]
37. Solymosi, F.; Erdőhelyi, A.; Bánsági, T. Infrared study of the surface interaction between H2 and CO_2 over rhodium on various supports. *J. Chem. Soc. Faraday Trans. 1 Phys. Chem. Condens. Phases* **1981**, *77*, 2645. [CrossRef]
38. Henderson, M.A.; Worley, S.D. An infrared study of the hydrogenation of carbon dioxide on supported rhodium catalysts. *J. Phys. Chem.* **1985**, *89*, 1417–1423. [CrossRef]
39. Fisher, I.A.; Bell, A.T. A Comparative Study of CO and CO_2 Hydrogenation over Rh/SiO_2. *J. Catal.* **1996**, *162*, 54–65. [CrossRef]
40. Tanaka, Y.; Iizuka, T.; Tanabe, K. Infrared spectroscopic study of CO and CO_2 adsorption on Rh-ZrO_2, Rh-Al_2O_3 and Rh-MgO. *J. Chem. Soc. Faraday Trans.* **1982**, *78*, 2215–2225. [CrossRef]
41. Heyl, D.; Rodemerck, U.; Bentrup, U. Mechanistic study of low-temperature CO_2 hydrogenation over modified Rh/Al_2O_3 catalysts. *ACS Catal.* **2016**, *6*, 6275–6284. [CrossRef]
42. Novák, É.; Fodor, K.; Szailer, T.; Oszkó, A.; Erdőhelyi, A. CO_2 hydrogenation on Rh/TiO_2 previously reduced at different temperatures. *Top. Catal.* **2002**, *20*, 107–117.
43. Tóth, M.; Kiss, J.; Oszkó, A.; Pótári, G.; László, B.; Erdőhelyi, A. Hydrogenation of carbon dioxide on Rh, Au and Au-Rh bimetallic clusters supported on titanate nanotubes, nanowires and TiO_2. *Top. Catal.* **2012**, *55*, 747–756.
44. Ruiz-García, J.R.; Fierro-Gonzalez, J.C.; Handy, B.E.; Hinojosa-Reyes, L.; Río, D.A.D.H.D.; Lucio-Ortiz, C.J.; Valle-Cervantes, S.; Flores-Escamilla, G.A. An In Situ Infrared Study of CO_2 Hydrogenation to Formic Acid by Using Rhodium Supported on Titanate Nanotubes as Catalysts. *ChemistrySelect* **2019**, *4*, 4206–4216.
45. Zhang, Z.L.; Kladi, A.; Verykios, X.E. Surface species formed during CO and CO_2 hydrogenation over Rh/TiO_2 (W6+) catalysts investigated by FTIR and mass-spectroscopy. *J. Catal.* **1995**, *156*, 37–50. [CrossRef]
46. Jacquemin, M.; Beuls, A.; Ruiz, P. Catalytic production of methane from CO_2 and H2 at low temperature: Insight on the reaction mechanism. *Catal. Today* **2010**, *157*, 462–466. [CrossRef]
47. Basini, L.; Marchionna, M.; Aragno, A. Drift and mass spectroscopic studies on the reactivity of rhodium clusters at the surface of polycrystalline oxides. *J. Phys. Chem.* **1992**, *96*, 9431–9441. [CrossRef]
48. Solymosi, F.; Erdőhelyi, A.; Kocsis, M. Surface interaction between H2 and CO_2 on Rh/Al_2O_3, studied by adsorption and infrared spectroscopic measurements. *J. Catal.* **1980**, *65*, 428–436. [CrossRef]
49. Beuls, A.; Swalus, C.; Jacquemin, M.; Hexen, G.; Karelovič, A.; Ruiz, P. Methanation of CO_2: Further insight into the mechanism over Rh/γ-Al_2O_3 catalyst. *Appl. Catal. B Environ.* **2012**, *113–114*, 2–10. [CrossRef]
50. Solymosi, F.; Pásztor, M.; Rákhely, G. Infrared studies of the effects of promoters on CO-induced structural changes in Rh. *J. Catal.* **1988**, *110*, 413–415. [CrossRef]
51. Trautmann, S.; Baerns, M. Infrared Spectroscopic Studies of CO Adsorption on Rhodium Supported by SiO_2, Al_2O_3, and TiO_2. *J. Catal.* **1994**, *150*, 335–344. [CrossRef]
52. Van't Blik, H.F.J.; Van Zon, J.B.A.D.; Huizinga, T.; Vis, J.C.; Koningsberger, D.C.; Prins, R. Structure of rhodium in an ultradispersed Rh/Al_2O_3 catalyst as studied by EXAFS and other techniques. *J. Am. Chem. Soc.* **1985**, *107*, 3139–3147. [CrossRef]
53. Amariglio, A.; Elbiache, A.; Amariglio, H. Effect of oxidizing pretreatments on the behavior of a rhodium powder in CO_2 chemisorption and methanation. *J. Catal.* **1986**, *98*, 355–366. [CrossRef]

54. Williams, K.J.; Boffa, A.B.; Salmeron, M.; Bell, A.T.; Somorjai, G.A. The kinetics of CO_2 hydrogenation on a Rh foil promoted by titania overlayers. *Catal. Lett.* **1991**, *9*, 415–426. [CrossRef]
55. Arandiyan, H.; Kani, K.; Wang, Y.; Jiang, B.; Kim, J.; Yoshino, M.; Rezaei, M.; Rowan, A.E.; Dai, H.; Yamauchi, Y. Highly Selective Reduction of Carbon Dioxide to Methane on Novel Mesoporous Rh Catalysts. *ACS Appl. Mater. Interfaces* **2018**, *10*, 24963–24968. [CrossRef]
56. Zheng, X.; Lin, Y.; Pan, H.; Wu, L.; Zhang, W.; Cao, L.; Zhang, J.; Zheng, L.; Yao, T. Grain boundaries modulating active sites in RhCo porous nanospheres for efficient CO_2 hydrogenation. *Nano Res.* **2018**, *11*, 2357–2365. [CrossRef]
57. Kohl, A.; Linsmeier, C.; Taglauer, E.; Knözinger, H. Influence of support and promotor on the catalytic activity of Rh/VOx/SiO_2 model catalysts. *Phys. Chem. Chem. Phys.* **2001**, *3*, 4639–4643. [CrossRef]
58. Boffa, A.; Lin, C.; Bell, A.T.; Somorjai, G.A. Promotion of CO and CO_2 Hydrogenation over Rh by Metal Oxides: The Influence of Oxide Lewis Acidity and Reducibility. *J. Catal.* **1994**, *149*, 149–158. [CrossRef]
59. Boffa, A.; Bell, A.T.; Somorjai, G.A. Vanadium Oxide Deposited on an Rh Foil: CO and CO_2 Hydrogenation Reactivity. *J. Catal.* **1993**, *139*, 602–610. [CrossRef]
60. Kusama, H.; Okabe, K.; Sayama, K.; Arakawa, H. CO_2 hydrogenation to ethanol over promoted Rh/SiO_2 catalysts. *Catal. Today* **1996**, *28*, 261–266. [CrossRef]
61. Inoue, T.; Iizuka, T.; Tanabe, K. Hydrogenation of carbon dioxide and carbon monoxide over supported rhodium catalysts under 10 bar pressure. *Appl. Catal.* **1989**, *46*, 1–9. [CrossRef]
62. Izumi, Y. Selective ethanol synthesis from carbon dioxide; roles of rhodium catalytic sites. *Platinum Met. Rev.* **1997**, *41*, 166–170.
63. Nozaki, F.; Sodesawa, T.; Satoh, S.; Kimura, K. Hydrogenation of carbon dioxide into light hydrocarbons at atmospheric pressure over Rh/Nb_2O_5 or Cu/SiO_2-Rh/Nb_2O_5 catalyst. *J. Catal.* **1987**, *104*, 339–346. [CrossRef]
64. Trovarelli, A.; Mustazza, C.; Dolcetti, G.; Kašpar, J.; Graziani, M. Carbon dioxide hydrogenation on rhodium supported on transition metal oxides. *Appl. Catal.* **1990**, *65*, 129–142. [CrossRef]
65. Solymosi, F.; Erdőhelyi, A.; Bánsági, T. Methanation of CO_2 on supported rhodium catalyst. *J. Catal.* **1981**, *68*, 371–382. [CrossRef]
66. Solymosi, F. Importance of the Electric Properties of Supports in the Carrier Effect. *Catal. Rev.* **1968**, *1*, 233–255. [CrossRef]
67. Iizuka, T.; Tanaka, Y.; Tanabe, K. Hydrogenation of carbon monoxide and carbon dioxide over supported rhodium catalysts. *J. Mol. Catal.* **1982**, *17*, 381–389. [CrossRef]
68. Iizuka, T.; Tanaka, Y.; Tanabe, K. Hydrogenation of CO and CO_2 over rhodium catalysts supported on various metal oxides. *J. Catal.* **1982**, *76*, 1–8. [CrossRef]
69. Karelovič, A.; Ruiz, P. Mechanistic study of low temperature CO_2 methanation over Rh/TiO_2 catalysts. *J. Catal.* **2013**, *301*, 141–153. [CrossRef]
70. Matsubu, J.C.; Yang, V.N.; Christopher, P. Isolated Metal Active Site Concentration and Stability Control Catalytic CO_2 Reduction Selectivity. *J. Am. Chem. Soc.* **2015**, *137*, 3076–3084. [CrossRef]
71. Ma, S.; Song, W.; Liu, B.; Zheng, H.; Deng, J.; Zhong, W.; Liu, J.; Gong, X.-Q.; Zhao, Z. Elucidation of the high CO_2 reduction selectivity of isolated Rh supported on TiO_2: A DFT study. *Catal. Sci. Technol.* **2016**, *6*, 6128–6136. [CrossRef]
72. Bando, K.K.; Ichikuni, N.; Soga, K.; Kunimori, K.; Arakawa, H.; Asakura, K. Characterization of Rh Particles and Li-Promoted Rh Particles in Y Zeolite during CO_2 Hydrogenation—A New Mechanism for Catalysis Controlled by the Dynamic Structure of Rh Particles and the Li Additive Effect. *J. Catal.* **2000**, *194*, 91–104. [CrossRef]
73. Deleitenburg, C.; Trovarelli, A. Metal-Support Interactions in Rh/CeO_2, Rh/TiO_2, and Rh/Nb_2O_5 Catalysts as Inferred from CO_2 Methanation Activity. *J. Catal.* **1995**, *156*, 171–174. [CrossRef]
74. Tauster, S.L.; Fung, S.C.; Garten, R.L. Strong metal-support interaction. Group 8 noble metals supported on TiO_2. *J. Am. Chem. Soc.* **1978**, *100*, 170–175. [CrossRef]
75. Matsubu, J.C.; Zhang, S.; DeRita, L.; Marinkovic, N.S.; Chen, J.G.; Graham, G.W.; Pan, X.; Christopher, P. Adsorbate-mediated strong metal–support interactions in oxide-supported Rh catalysts. *Nat. Chem.* **2017**, *9*, 120–127. [CrossRef] [PubMed]
76. Chandler, B. D Strong metal-support interactions; An external layer of complexity. *Nat. Chem.* **2017**, *9*, 108–109. [CrossRef] [PubMed]

77. Solymosi, F.; Tombácz, I.; Koszta, J. Effects of variation of electric properties of TiO_2 support on hydrogenation of CO and CO_2 over Rh catalysts. *J. Catal.* **1985**, *95*, 578–586. [CrossRef]
78. Zhang, Z.; Kladi, A.; Verykios, X. Effects of Carrier Doping on Kinetic Parameters of CO_2 Hydrogenation on Supported Rhodium Catalysts. *J. Catal.* **1994**, *148*, 737–747. [CrossRef]
79. Karelovič, A.; Ruiz, P. CO_2 hydrogenation at low temperature over Rh/γ-Al_2O_3 catalysts: Effect of the metal particle size on catalytic performances and reaction mechanism. *Appl. Catal. B Environ.* **2012**, *113–114*, 237–249.
80. Kurakata, H.; Izumi, Y.; Aika, K.I. Ethanol synthesis from carbon dioxide on TiO_2-supported [Rh10Se] catalyst. *Chem. Commun.* **1996**, *389*, 389–390. [CrossRef]
81. Szailer, T.; Novák, É.; Oszkó, A.; Erdőhelyi, A. Effect of H2S on the hydrogenation of carbon dioxide over supported Rh catalysts. *Top. Catal.* **2007**, *46*, 79–86. [CrossRef]
82. Kusama, H.; Bando, K.K.; Okabe, K.; Arakawa, H. Effect of metal loading on CO_2 hydrogenation reactivity over Rh/SiO_2 catalysts. *Appl. Catal. A Gen.* **2000**, *197*, 255–268. [CrossRef]
83. Kusama, H.; Bando, K.K.; Okabe, K.; Arakawa, H. CO_2 hydrogenation reactivity and structure of Rh/SiO_2 catalysts prepared from acetate, chloride and nitrate precursors. *Appl. Catal. A Gen.* **2001**, *205*, 285–294. [CrossRef]
84. Ichikawa, S. Reactive chemisorption and methanation of carbon dioxide on rhodium particles approaching atomic dispersion. *J. Mol. Catal.* **1989**, *53*, 53–65. [CrossRef]
85. Trovarelli, A.; Deleitenburg, C.; Dolcetti, G.; Lorca, J. CO_2 Methanation Under Transient and Steady-State Conditions over Rh/CeO_2 and CeO_2-Promoted Rh/SiO_2: The Role of Surface and Bulk Ceria. *J. Catal.* **1995**, *151*, 111–124. [CrossRef]
86. Arakawa, H.; Takeuchi, K.; Matsuzaki, T.; Sugi, Y. Effect of the metal dispersion on the activity and selectivity of Rh/SiO_2 catalyst for high pressure CO hydrogenation. *Chem. Lett.* **1984**, *13*, 1607–1610. [CrossRef]
87. Bhasin, M.M.; Bartley, W.J.; Ellgen, P.C.; Wilson, T.P. Synthesis gas conversion over supported rhodium and rhodium-iron catalysts. *J. Catal.* **1978**, *54*, 120–128. [CrossRef]
88. Kusama, H.; Okabe, K.; Sayama, K.; Arakawa, H. Ethanol synthesis by catalytic hydrogenation of CO_2 over Rh-Fe/SiO_2 catalysts. *Energy* **1997**, *22*, 343–348. [CrossRef]
89. Arakawa, H. Research and development on new synthetic routes for basic chemicals by catalytic hydrogenation of CO_2. *Stud. Surf. Sci. Catal.* **1998**, *114*, 19–30.
90. Gogate, M.R.; Davis, R.J. Comparative study of CO and CO_2 hydrogenation over supported Rh–Fe catalysts. *Catal. Commun.* **2010**, *11*, 901–906. [CrossRef]
91. Kusama, H.; Okabe, K.; Sayama, K.; Arakawa, H. Alcohol synthesis by catalytic hydrogenation of CO_2 over Rh-Co/SiO_2. *Appl. Organometal. Chem.* **2000**, *14*, 836–840. [CrossRef]
92. Kusama, H.; Okabe, K.; Arakawa, H. Characterization of Rh-Co/SiO_2 catalysts for CO_2 hydrogenation with TEM, XPS and FT-IR. *Appl. Catal. A Gen.* **2001**, *207*, 85–94. [CrossRef]
93. Gronchi, P.; Marengo, S.; Mazzocchia, C.; Tempesti, E.; Del Rosso, R. On the formation of oxygenated products by CO hydrogenation with lanthana promoted rhodium catalysts. *React. Kinet. Catal. Lett.* **1997**, *60*, 79–88. [CrossRef]
94. Ikehara, N.; Hara, K.; Satsuma, A.; Hattori, T.; Murakami, Y. Unique Temperature Dependence of Acetic Acid Formation in CO_2 Hydrogenation on Ag-promoted Rh/SiO_2 Catalyst. *Chem. Lett.* **1994**, *23*, 263–264. [CrossRef]
95. Bowker, M. On the mechanism of ethanol synthesis on rhodium. *Catal. Today* **1992**, *15*, 77–100. [CrossRef]
96. Ding, Y.-H.; Huang, W.; Wang, Y.-G. Direct synthesis of acetic acid from CH_4 and CO_2 by a step-wise route over Pd/SiO_2 and Rh/SiO_2 catalysts. *Fuel Process. Technol.* **2007**, *88*, 319–324. [CrossRef]
97. Erdőhelyi, A.; Kocsis, M.; Bánsági, T.; Solymosi, F. Hydrogenation of CO_2 on Rh/Al_2O_3. *Acta Chim. Acad. Sci. Hung.* **1982**, *111*, 591–605.
98. Bowker, M.; Cassidy, T.; Ashcroft, A.; Cheetham, A. The Methanation of CO and CO_2 over a Rh/Al_2O_3 Catalyst Using a Pulsed-Flow Microreactor. *J. Catal.* **1993**, *143*, 308–313. [CrossRef]
99. Martin, N.M.; Hemmingsson, F.; Wang, X.; Merte, L.R.; Hejral, U.; Gustafson, J.; Skoglundh, M.; Meira, D.M.; Dippel, A.-C.; Gutowski, O.; et al. Structure–function relationship during CO_2 methanation over Rh/Al_2O_3 and Rh/SiO_2 catalysts under atmospheric pressure conditions. *Catal. Sci. Technol.* **2018**, *8*, 2686–2696. [CrossRef]

100. Tripol'skii, A.I. Effect of modifying additive to rhodium–containing catalyst on the kinetics of CO_2 hydrogenation. *Theor. Exp. Chem.* **2011**, *47*, 331–336.
101. Büchel, R.; Baiker, A.; Pratsinis, S.E. Effect of Ba and K addition and controlled spatial deposition of Rh in Rh/Al_2O_3 catalysts for CO_2 hydrogenation. *Appl. Catal. A Gen.* **2014**, *477*, 93–101.
102. Karelovič, A.; Ruiz, P. Improving the Hydrogenation Function of Pd/γ-Al_2O_3 Catalyst by Rh/γ-Al_2O_3 Addition in CO_2 Methanation at Low Temperature. *ACS Catal.* **2013**, *3*, 2799–2812. [CrossRef]
103. Swalus, C.; Jacquemin, M.; Poleunis, C.; Bertrand, P.; Ruiz, P. CO_2 methanation on Rh/γ-Al_2O_3 catalyst at low temperature: "In situ" supply of hydrogen by Ni/activated carbon catalyst. *Appl. Catal. B Environ.* **2012**, *125*, 41–50. [CrossRef]
104. Martin, N.M.; Hemmingsson, F.; Schaefer, A.; Ek, M.; Merte, L.R.; Hejral, U.; Gustafson, J.; Skoglundh, M.; Dippel, A.-C.; Gutowski, O.; et al. Structure–function relationship for CO_2 methanation over ceria supported Rh and Ni catalysts under atmospheric pressure conditions. *Catal. Sci. Technol.* **2019**, *9*, 1644–1653. [CrossRef]
105. Kai, T.; Matsumura, T.; Takahashi, T. The effect of support structure on CO_2 hydrogenation over a rhodium catalyst supported on niobium oxide. *Catal. Lett.* **1992**, *16*, 129–135. [CrossRef]
106. Kobayashi, M.; Kanno, T.; Konishi, Y.; Ohashi, H. Dynamic kinetics of the common intermediates formed in CO and CO_2 hydrogenation on Rh/MgO. *Chem. Eng. Commun.* **1988**, *71*, 189–193. [CrossRef]
107. Reyes, P.; Concha, I.; Pecchi, G.; Fierro, J. Changes induced by metal oxide promoters in the performance of Rh–Mo/ZrO2 catalysts during CO and CO_2 hydrogenation. *J. Mol. Catal. A Chem.* **1998**, *129*, 269–278. [CrossRef]
108. Boaro, M.; Colussi, S.; Trovarelli, A. Ceria-based materials in hydrogenation and reforming reactions for CO_2 valorization. *Front. Chem.* **2019**, *7*, 28. [CrossRef]
109. Varga, E.; Pusztai, P.; Oszkó, A.; Baán, K.; Erdőhelyi, A.; Kónya, Z.; Kiss, J. Stability and Temperature-Induced Agglomeration of Rh Nanoparticles Supported by CeO_2. *Langmuir* **2016**, *32*, 2761–2770. [CrossRef]
110. Kai, T.; Yamasaki, Y.; Takahashi, T.; Masumoto, T.; Kimura, H. Increase in the thermal stability during the methanation of CO_2 over a Rh catalyst prepared from an amorphous alloy. *Can. J. Chem. Eng.* **1998**, *76*, 331–335. [CrossRef]
111. Kishida, M.; Fujita, T.; Umakoshi, K.; Ishiyama, J.; Nagata, H.; Wakabayashi, K. Novel preparation of metal-supported catalysts by colloidal microparticles in a water-in-oil microemulsion; catalytic hydrogenation of carbon dioxide. *J. Chem. Soc. Chem. Commun.* **1995**, 763–764. [CrossRef]
112. Yan, B.; Wu, Q.; Cen, J.; Timoshenko, J.; Frenkel, A.I.; Su, D.; Chen, X.; Parise, J.B.; Stach, E.; Orlov, A.; et al. Highly active sub-nanometer Rh clusters derived from Rh-doped SrTiO3 for CO_2 reduction. *Appl. Catal. B Environ.* **2018**, *237*, 1003–1011. [CrossRef]
113. Bando, K.K.; Soga, K.; Kunimori, K.; Ichikuni, N.; Okabe, K.; Kusama, H.; Sayama, K.; Arakawa, H. CO_2 hydrogenation activity and surface structure of zeolite-supported Rh catalysts. *Appl. Catal. A Gen.* **1998**, *173*, 47–60. [CrossRef]
114. Wang, C.; Guan, E.; Wang, L.; Chu, X.; Wu, Z.; Zhang, J.; Yang, Z.; Jiang, Y.; Zhang, L.; Meng, X.; et al. Product Selectivity Controlled by Nanoporous Environments in Zeolite Crystals Enveloping Rhodium Nanoparticle Catalysts for CO_2 Hydrogenation. *J. Am. Chem. Soc.* **2019**, *141*, 8482–8488. [CrossRef] [PubMed]
115. Bando, K.K.; Soga, K.; Kunimori, K.; Arakawa, H. Effect of Li additive on CO_2 hydrogenation reactivity of zeolite supported Rh catalysts. *Appl. Catal. A Gen.* **1998**, *175*, 67–81. [CrossRef]
116. Lavalley, J. Infrared spectrometric studies of the surface basicity of metal oxides and zeolites using adsorbed probe molecules. *Catal. Today* **1996**, *27*, 377–401. [CrossRef]
117. Szanyi, J.; Kwak, J.H. Dissecting the steps of CO_2 reduction: 1. The interaction of CO and CO_2 with γ-Al_2O_3: An in situ FTIR study. *Phys. Chem. Chem. Phys.* **2014**, *16*, 15117–15125. [CrossRef] [PubMed]
118. Solymosi, F.; Bánsági, T.; Erdőhelyi, A. Infrared study of the reaction of adsorbed formate ion with H2 on supported Rh catalysts. *J. Catal.* **1981**, *72*, 166–169. [CrossRef]
119. Benitez, J.J.; Carrizosa, I.; Odriozola, J.A. HCOOH hydrogenation over lanthanide-oxide-promoted $Rh/A1_2O_3$ catalysts. *Appl. Surf. Sci.* **1993**, *68*, 565–573. [CrossRef]
120. Worley, S.D.; Rice, C.A.; Curtis, C.V.; Guin, J.A. Effect of support material on Rh catalysts. *J. Phys Chem.* **1982**, *86*, 2714–2717. [CrossRef]
121. Solymosi, F.; Lancz, M. Effects of different surface species on the infrared spectrum of CO adsorbed on Rh/Al_2O_3. *J. Chem. Soc. Faraday Trans. 1 Phys. Chem. Condens. Phases* **1986**, *82*, 883. [CrossRef]

122. Henderson, M.A.; Worley, S.D. An infrared study of isotopic exchange during methanation over supported rhodium catalysts: An inverse spillover effect. *J. Phys. Chem.* **1985**, *89*, 392–394. [CrossRef]
123. Iizuka, T.; Tanaka, Y. Dissociative adsorption of CO_2 on supported rhodium catalyst: Comment on surface interaction between H_2 and CO_2 on Rh-Al_2O_3. *J. Catal.* **1981**, *70*, 440–441. [CrossRef]
124. Benitez, J.J.; Alvero, R.; Carrizosa, I.; Odriozola, J.A. "In situ" DRIFTS study of adsorbed species in the hydrogenation of carbon oxides. *Catal. Today* **1991**, *9*, 53–60. [CrossRef]
125. Yoshida, H.; Narisawa, S.; Fujita, S.-I.; Ruixia, L.; Arai, M. In situ FTIR study on the formation and adsorption of CO on alumina-supported noble metal catalysts from H2 and CO_2 in the presence of water vapor at high pressures. *Phys. Chem. Chem. Phys.* **2012**, *14*, 4724. [CrossRef] [PubMed]
126. Bradford, M.C.J.; Vannice, M.A. Metal-support interactions during the CO_2 reforming of CH_4 over model TiO_x/Pt catalysts. *Catal. Lett.* **1997**, *48*, 31–38. [CrossRef]
127. Stevenson, S.A.; Lisitsyn, A.; Knoezinger, H. Adsorption of carbon monoxide on manganese-promoted rhodium/silica catalysts as studied by infrared spectroscopy. *J. Phys. Chem.* **1990**, *94*, 1576–1581. [CrossRef]
128. Chuang, S.S.C.; Stevens, R.W., Jr.; Khatri, R. Mechanism of C_{2+} oxygenate synthesis on Rh catalysts. *Top. Catal.*, **2005**, *32*, 225–232. [CrossRef]
129. Raskó, J.; Kecskés, T.; Kiss, J. Adsorption and reaction of formaldehyde on TiO_2-supported Rh catalysts studied by FTIR and mass spectrometry. *J. Catal.* **2004**, *226*, 183–191. [CrossRef]
130. Pan, Q.; Peng, J.; Wang, S.; Wang, S. In situ FTIR spectroscopic study of the CO_2 methanation mechanism on Ni/$Ce_{0.5}Zr_{0.5}O_2$. *Cat. Sci. Technol.* **2014**, *4*, 502–509. [CrossRef]
131. Wang, F.; He, S.; Chen, H.; Wang, B.; Zheng, L.; Wei, M.; Evans, D.G.; Duan, X. Active Site Dependent Reaction Mechanism over Ru/CeO_2 Catalyst toward CO_2 Methanation. *J. Am. Chem. Soc.* **2016**, *138*, 6298–6305. [CrossRef]
132. Erdőhelyi, A.; Solymosi, F. Effects of the support on the adsorption and dissociation of CO and on the reactivity of surface carbon on Rh catalysts. *J. Catal.* **1983**, *84*, 446–460. [CrossRef]
133. Solymosi, F.; Tombácz, I.; Kocsis, M. Hydrogenation of CO on supported Rh catalysts. *J. Catal.* **1982**, *75*, 78–93. [CrossRef]